ผลของเอเซียติโคไซด์ที่มีต่อการเกิดอนุพันธ์ออกซิเจนที่ว่องไวจากการเหนี่ยวนำโดย 4 -ไฮดรอกซี - 2 - โนนีนัลในเซลล์อีซีวี - 304

นายวิศรุต บูรณสัจจะ

วิทยานิพนธ์นี้เป็นส่วนหนึ่งของการศึกษาตามหลักสูตรปริญญาเภสัชศาสตรมหาบัณฑิต
สาขาวิชาสรีรวิทยา ภาควิชาเภสัชวิทยาและสรีรวิทยา
คณะเภสัชศาสตร์ จุฬาลงกรณ์มหาวิทยาลัย
ปีการศึกษา 2551

EFFECT OF ASIATICOSIDE ON GENERATION OF REACTIVE OXYGEN SPECIES BY INDUCTION OF 4-HYDROXY-2-NONENAL IN ECV-304 CELLS

Mr. Visarut Buranasudja

A Thesis Submitted in Partial Fulfillment of the Requirements
for the Degree of Master of Science in Pharmacy Program in Physiology
Department of Pharmacology and Physiology
Faculty of Pharmaceutical Sciences
Chulalongkorn University
Academic Year 2008

Thesis Title	EFFECT OF ASIATICOSIDE ON GENERATION OF REACTIVE OXYGEN SPECIES BY INDUCTION OF 4-HYDROXY- 2 -NONENAL IN ECV-304 CELLS
By	Mr. Visarut Buranasudja
Field of Study	Physiology
Advisor	Associate Professor Vimolmas Lipipun, Ph.D.
Co-Advisor	Associate Professor Rupporn Kittiwatchara Pithi Chanvorachote, Ph.D.

Accepted by the Faculty of Pharmaceutical Sciences, Chulalongkorn University in Partial Fulfillment of the Requirements for the Master's Degree

…….....Dean of the Faculty of Pharmaceutical Sciences

(Associate Professor Pornpen Pramyothin, Ph.D.)

THESIS COMMITTEE

…….. Chairman

(Associate Professor Somsong Lawanprasert, Ph.D.)

…….……. Advisor

(Associate Professor Vimolmas Lipipun, Ph.D.)

…….. Co-Advisor

(Pithi Chanvorachote, Ph.D.)

…….. Examiner

(Professor Ratree Sudsuang, Ph.D.)

…….. External Examiner

(Associate Professor Uthai Sotanaphun, Ph.D.)

วิศรุต บูรณสัจจะ: ผลของเอเซียติโคไซด์ที่มีต่อการเกิดอนุพันธ์ออกซิเจนที่ว่องไวจากการเหนี่ยวนำโดย 4-ไฮดรอกซี-2-โนนีนัลในเซลล์อีซีวี-304 (EFFECT OF ASIATICOSIDE ON GENERATION OF REACTIVE OXYGEN SPECIES BY INDUCTION OF 4-HYDROXY-2-NONENAL IN ECV-304 CELLS) อ.ที่ปรึกษาวิทยานิพนธ์หลัก : รศ.ดร. วิมลมาศ ลิปีพันธ์, อ.ที่ปรึกษาวิทยานิพนธ์ร่วม : รศ. รับพร กิตติวัชร, อ.ดร. ปิติ จันทร์วรโชติ, 70 หน้า.

4-Hydroxy-2-nonenal (4-HNE) เป็นสารในกลุ่มแอลดีไฮด์ที่พบได้มากที่สุดจากกระบวนการ lipid peroxidation โดย 4-HNE มีความเกี่ยวข้องกับกระบวนการเกิดพยาธิสภาพในหลายโรค ซึ่งพบว่าเกี่ยวข้องกับการเหนี่ยวนำการสร้างอนุพันธ์ออกซิเจนที่ว่องไวภายในเซลล์ วัตถุประสงค์ของงานวิจัยนี้เพื่อศึกษากลไกความเป็นพิษระดับชีววิทยาโมเลกุลของ 4-HNE ต่อเซลล์ ECV-304 รวมทั้งศึกษาผลของเอเซียติโค-ไซด์ซึ่งเป็นสารสำคัญจากสารสกัดใบบัวบกต่อการเกิดพิษของ 4-HNE จากผลการศึกษาด้วยวิธี MTT พบว่าความเป็นพิษต่อเซลล์ของ 4-HNE เพิ่มขึ้นเป็นสัดส่วนโดยตรงกับความเข้มข้น จากนั้นทำการศึกษารูปแบบการตายของเซลล์โดยวิธีการย้อมสี Hoechst 33342 และ propidium iodide พบว่าเซลล์มีการตายแบบอะพอพโทสิสและเนโครสิสเพิ่มขึ้นอย่างมีนัยสำคัญ ($P < 0.05$) หลังจากได้รับ 4-HNE เป็นเวลา 12 ชั่วโมง และเมื่อเติมสารต้านอนุมูลอิสระ N-acetyl-L-cysteine หรือ glutathione จะทำให้การเกิดพิษต่อเซลล์ของ 4-HNE ลดลงอย่างมีนัยสำคัญ ($P < 0.05$) เมื่อวิเคราะห์ด้วยวิธี MTT นอกจากนี้ยังพบว่าการเติมสารต่อต้านอนุมูลอิสระจะลดการตายของเซลล์แบบอะพอพโทสิสและเนโครสิสซึ่งถูกเหนี่ยวนำโดย 4-HNE อย่างมีนัยสำคัญ ($P < 0.05$) จากนั้นเมื่อทำการวัดปริมาณอนุพันธ์ออกซิเจนที่ว่องไวภายในเซลล์ที่ได้รับ 4-HNE โดยใช้สีย้อมที่มีความจำเพาะต่ออนุพันธ์ออกซิเจนที่ว่องไวคือ 2',7' – dichlorodihydrofluorecein diacetate และวิเคราะห์ด้วยวิธีโฟลไซโตเมทรีพบว่า 4-HNE เหนี่ยวนำให้เกิดกระบวนการสร้างอนุพันธ์ออกซิเจนที่ว่องไวเพิ่มขึ้นอย่างมีนัยสำคัญ ($P < 0.05$) ดังนั้นจากการศึกษาข้างต้นพบว่าอนุพันธ์ออกซิเจนที่ว่องไวน่าจะมีความเกี่ยวข้องต่อการเกิดพิษของ 4-HNE อย่างไรก็ตามเอเซียติโคไซด์ ซึ่งเป็นสารที่มีรายงานวิจัยว่าเป็นสารต่อต้านอนุมูลอิสระ และในงานวิจัยนี้พบว่าเอเซียติโคไซด์มีฤทธิ์ต้านอนุมูลอิสระเฉพาะในระดับความเข้มข้นที่สูง (200 µM) แสดงให้เห็นว่าฤทธิ์ดังกล่าวอาจจะไม่มีความเกี่ยวข้องต่อกระบวนการป้องกันอันตรายต่อเซลล์ที่เกิดจาก 4-HNE ส่วนกระบวนการป้องกันอันตรายต่อเซลล์ที่เกิดจาก 4-HNE ของเอเซียติโคไซด์ที่แน่นอนจะต้องทำการศึกษาต่อไป

ภาควิชา.....เภสัชวิทยาและสรีรวิทยา.....ลายมือชื่อนิสิต.....

สาขาวิชา.....สรีรวิทยา.....ลายมือชื่ออ.ที่ปรึกษาวิทยานิพนธ์หลัก.....

ปีการศึกษา...2551.....ลายมือชื่ออ.ที่ปรึกษาวิทยานิพนธ์ร่วม.....

ลายมือชื่ออ.ที่ปรึกษาวิทยานิพนธ์ร่วม.....

4976594033 : MAJOR PHYSIOLOGY
KEYWORDS: 4-hydroxy-2-nonenal / ECV-304 cells / Reactive oxygen species / Asiaticoside

VISARUT BURANASUDJA: EFFECT OF ASIATICOSIDE ON GENERATION OF REACTIVE OXYGEN SPECIES BY INDUCTION OF 4-HYDROXY-2-NONENAL IN ECV-304 CELLS. THESIS ADVISOR: ASSOC. PROF. VIMOLMAS LIPIPUN, Ph. D., THESIS CO-ADVISOR: ASSOC. PROF. RUPPORN KITTIWATCHARA,
PITHI CHANVORACHOTE, Ph.D., 70 pp.

4-hydroxy-2-nonenal (4-HNE), the most abundant aldehyde product of lipid peroxidation, was shown to exert several effects on pathological processes. Its effects were shown to be tightly associated with an ability to induce intracellular reactive oxygen species (ROS) generation. The purposes of this study were to elucidate the possible cytotoxic role of 4-HNE and underlying mechanisms on ECV-304 cells. Moreover, this study investigated the protective effect of asiaticoside, the major active component of *Centella asiatica* (Linn.), against 4-HNE mediated cytotoxicity. Exposure with 4-HNE decreased cell viability in a concentration dependent manner over a wide range concentrations (0-40 μM) analyzed by MTT assay. In addition, Hoechst 33342 and propidium iodide staining assay showed a significant increase ($P < 0.05$) in apoptotic and necrotic cells at 12 hours. Addition of antioxidant, N-acetyl-L-cysteine (NAC) or glutathione (GSH), significantly inhibited ($P < 0.05$) 4-HNE induced cytotoxicity measured by MTT assay, apoptotic cell death analyzed by Hoechst 33342 staining assay, and necrotic cell death determined by propidium iodide staining assay. Flow cytometric analysis of ROS-specific 2', 7' – dichlorodihydrofluorecein diacetate fluorescent dye indicated that 4-HNE treatment strongly significant up-regulated ($P < 0.05$) intracellular ROS, suggesting the involvement of ROS on 4-HNE induced cytotoxicity. However, asiaticoside which has been reported to be an antioxidant showed antioxidant effect only at high concentrations (200 μM) in this study. These findings provided evidence that antioxidant effect of asiaticoside might not be involved in the protection of ECV-304 cells against 4-HNE induced toxicity. Nevertheless, the precise mechanisms of asiaticoside in protection of 4-HNE induced cytotoxicity remain to be defined.

Department…Pharmacology and Physiology…Student's signature: …….

Field of study…….Physiology……..Advisor's signature: …….

Academic year……2008……...Co-Advisor's signature: ……...

Co-Advisor's signature: ……

ACKNOWLEDGEMENTS

My heartfelt thanks to my advisor, Associate Professor Dr. Vimolmas Lipipun, my co-advisors, Associate Professor Rupporn Kittiwatchara and Dr. Pithi Chanvorachote, from the very first day of my study in Physiology program have given me the invaluable advices, supervision, encouragement throughout this study.

I am very much obliged and honored to the members of the Thesis Committee for their supportive attitude, constructive criticisms and for their invaluable discussions over my thesis.

I would like to special thank to Assistant Professor Dr. Surachai Unchern of the Department of Pharmacology and Physiology, Faculty of Pharmaceutical Sciences, Chulalongkorn University for graciously providing ECV-304 cells.

I would like to express my deep appreciated to Noppadol Sa-Ard-Iam of the Department of Periodontology, Faculty of Dentistry, Chulalongkorn University for his excellent assistance in flow cytometry techniques.

This work was financially supported by Graduate Thesis Grant, from Graduate school, Chulalongkorn University.

It would not be completed without expressing my sincere gratitude to my parents for their love, understanding, moral support and tremendous encouragements throughout my life.

CONTENTS

Page

LIST OF FIGURES

Figure **Page**

LIST OF ABBREVIATIONS

ADP	adenosine diphosphate
ANOVA	analysis of variance
ATP	adenosine triphosphate
CoQ	coenzyme Q
COPD	chronic obstructive pulmonary disease
DCF	2',7' – dichlorofluorecein
$DCFH_2$-DA	2',7' – dichlorodihydrofluorescein diacetate
DMEM	Dulbecco's modified Eagle's medium
DNA	deoxyribonucleic acid
$\bar{e}$	electron
et al.	et alii, and others
FA-OOH	fatty acid hydroperoxides
FAD	flavin adenine dinucleotide
$FADH_2$	reduced form of flavin adenine dinucleotide
FBS	fetal bovine serum
FEV_1	force expiratory in 1 second
Fe^{2+}	ferrous iron
Fe^{3+}	ferric iron
γ-GCS	gamma-glutamylcysteine synthetase
GSH	glutathione
GPxs	glutathione peroxidases
GSTs	glutathione S–transferases
4-HNE	4-hydroxy-2-nonenal
H^+	hydrogen ion
H_2O_2	hydrogen peroxide
HOO•	hydroperoxyl radical
JNK	c-Jun N-terminal protein kinase
LDL	low density lipoprotein
LOOH	fatty acid hydroperoxide
MDA	malondialdehyde

μg	microgram (s)
μM	micromolar
ml	milliliter (s)
mM	millimolar
MTT	3-(4,5-dimethylthiazol-2-yl)-2,5-diphenyltetrazolium bromide
NAC	N-acetyl-L-cysteine
NAD^+	nicotinamide adenine dinucleotide
NADH	reduced form of nicotinamide adenine dinucleotide
NADPH	reduced form of nicotinamide adenine dinucleotide phosphate
$O_2•^-$	superoxide anion radical
8-OH-G	8-hydroxyguanosine
OH^-	hydroxyl anion
•OH	hydroxyl radical
PBS	phosphate buffered saline
PI	propidium iodide
Pi	phosphate
PL-OOH	phospholipid hydroperoxides
PUFA	polyunsaturated fatty acid
p*K*a	a logarithmic measure of the acid dissociation constant
ROS	reactive oxygen species
ROO•	peroxyl radical
RNA	ribonucleic acid
S.E.M.	standard error of the mean
SOD	superoxide dismutase
-SH	thiol group
TBARS	thiobarbitoric acid reactive substance
TGF-β_1	transforming growth factor-beta 1
XD	xanthine dehydrogenase
XO	xanthine oxidase

XOR	xanthine oxidoredutase

CHAPTER I
INTRODUCTION

Oxidative stress has been concerned as a component of molecular mechanisms of tissue damage found in number of pathologies. One of the most important oxidative mechanisms which play a critical role in cell and tissue damages is known as lipid peroxidation. This reaction is initiated and propagated by reactive oxygen species formed by intracellular oxidative stresses, and damage membrane of the cells **(1, 2)**. Lipid peroxidation reaction not only causes a severe membrane damage leading to cell death, but also generates several resulted radicals and toxic metabolites which in turn further propagate oxidative stresses to the surrounding cells and tissues. One of the major aldehydic end products of lipid peroxidation is 4-hydroxy-2-nonenal (4-HNE). 4-HNE has been postulated to play a role in several disease states including, atherosclerosis **(3-6)**, cancer **(7)**, chronic obstructive pulmonary disease **(8-12)**, and neurological disorders **(13-23)**. Increasing number of evidence indicates that 4-HNE induced cytotoxicity through an increased intracellular production of reactive oxygen species (ROS) **(24-28)**. However, the cytotoxic effect of 4-HNE and its underlying mechanisms in regulation of vascular cell and tissue damage are largely unknown. Thus, the present study used the endothelial ECV-304 cells as a representative model in investigation of cytotoxicity and mechanisms of action of 4-HNE.

Centella asiatica (L.) Urban (family Umbelliferae) has been used in folk medicine in many Asian countries. This plant is claimed to posses anti-inflammatory **(29)**, memory improvement **(30, 31)** and anticancer activity **(32)**. Based on the hypothesis of free radical mediated toxicity, *Centella asiatica* has been reported to have anti-lipid peroxidative **(33)** and antioxidative activities **(30, 31, 33-38)**. Its active components include several pentacyclic triterpine derivatives **(39)**. Asiaticoside is the most abundant triterpene glycoside, which has been shown to promote collagen formation and angiogenesis in wound healing **(40)**. Moreover, asiaticoside also has been reported to enhance induction of enzymatic and non-enzymatic antioxidant levels **(41)**.

Nevertheless, the protective role of asiaticoside against 4-HNE induced cell damage is still not elucidated.

In summary, the purposes of this study is to determine the role of 4-HNE and its underlying mechanism on ECV-304 cell damage as well as investigate the protective effect of asiaticoside against 4-HNE induced cytotoxicity.

CHAPTER II
LITERATURE REVIEW

1. *Centella asiatica* (Linn.) Urban

Figure 1 *Centella asiatica* (Linn.) Urban

Centella asiatica (Gotu kola, Asiatic pennywort, Buabok) is a perennial herbaceous plant of the family Umbelliferae, native to India, Japan, China, Indonesia, South Africa, Sri Lanka, and the South Pacific. It is tasteless and odorless and thrives in and around water. It has small fan-shaped green leaves with white or light purple-to-pink flowers, and it bears small oval fruit (Figure 1).

In an Indian system of medicine, Ayurveda, *C. asiatica* has been used for different ailments like headache, body aches, insanity, asthma, leprosy, ulcers, eczemas

and wound healing. In the course of pharmacological studies, the plant showed anti-inflammatory **(29)**, memory improvement **(30, 31)** and anticancer activity **(32)**. Moreover, several studies have shown that *C. asiatica* inhibited free radical generation, and acted as free radical scavengers, antioxidants **(30, 31, 33-38)**.

The major active components of *C. asiatica* are triterpene saponins, asiaticoside and madecassoside, and their aglycones, asiatic acid and medecassic acid **(39)**. It is also contains essential oils and other volatile constituents. This plant contains other saponins and triterpene acids, namely, cettilic acid, cetelloside, brahmoside, brahminoside, brahmic acid, isobrahmic acid, etc.

Asiaticoside is the most essential ingredient and founded to be the most content extracted from *C. asiatica* (the structure shown in Figure 2).

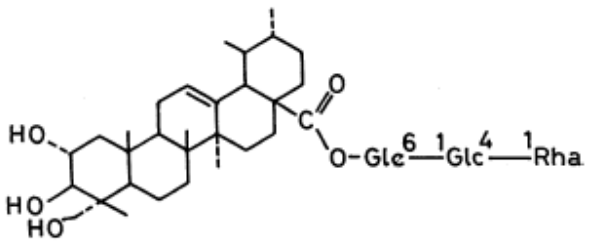

Figure 2 Structure of asiaticoside **(40)**

2. Pharmacological activities of asiaticoside

2.1 Antioxidant

Topical administration of 0.2% solution of asiaticoside twice daily for 7 days to skin wounds in rats enhanced induction enzymatic and non-enzymatic antioxidant levels, including superoxide dismutase (35%), catalase (67%), glutathione peroxidase (49%), vitamin E (77%) and ascorbic acid (37%), in newly form tissue at an initial stage of healing. It also resulted in a several fold decrease in lipid peroxide levels (69%) as measured in terms of thiobarbitoric acid reactive substance (TBARS) **(41)**.

2.2 Anxiolytic

Using elevated plus maze, open field, social interaction, locomotor activity, punished drinking, and novel cage tests on rats, Wijeweera, P., et al. (2006) suggested that asiaticoside had anxiolytic activity **(42)**.

2.3 Wound healing

Shukla, A., et al. (1999) found that the administration of a topical solution of 0.2% asiaticoside in guinea pig punch wounds produced 56% increase in hydroxyproline, 57% increase in tensile strength, increased collagen content and better epithelisation than controls. They also demonstrated that topical application of 0.4% solution of asiaticoside over punch wounds in streptozocin diabetic rats, in which healing is delayed, increased hydroxyproline content, tensile strength, collagen content and epithelisation. Moreover, asiaticoside promoted angiogenesis in the chick chorioallantoic model at 40 μg **(40)**.

3. The mitochondrion

The mitochondrion is the site of eukaryotic oxidative metabolism. Mitochondria contain pyruvate dehydrogenase, the citric acid cycle enzymes, the enzymes catalyzing fatty acid oxidation, and the enzymes and redox proteins involved in electron transport and oxidative phosphorylation. It is therefore with good reason that the mitochondrion is often described as the cell's "power plant".

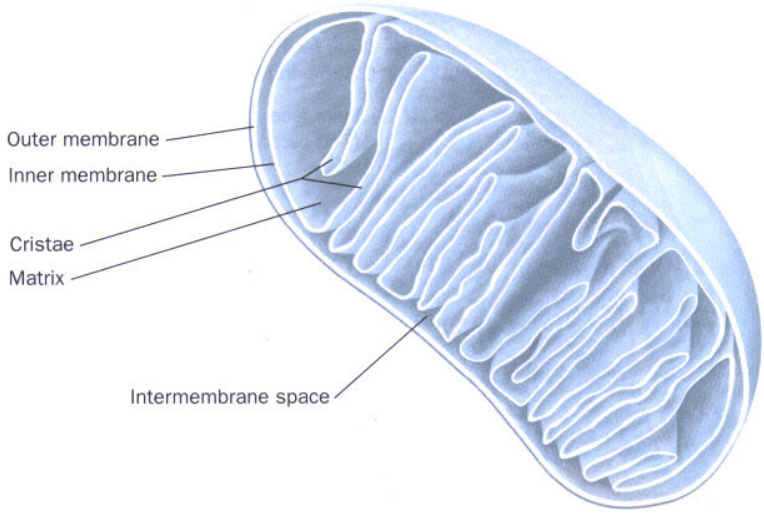

Figure 3 Mitochondrion **(43)**

Mitochondria vary in size and shape, depending on their source and metabolic state. A eukaryotic cell typically contains about 2000 mitochondria, which occupy roughly one-fifth of its total cell volume. A mitochondrion is bounded by a smooth outer membrane and contains as extensively invaginated inner membrane (Figure 3). The number of invaginations, called cristae, reflects the respiratory activity of the cell. The proteins mediating electron transport and oxidative phosphorylation are bound in the inner mitochondrial membrane.

The inner membrane divides the mitochondrion into two compartments, the inner membrane space and the internal matrix. The matrix is a gel-like solution that contains extremely high concentrations of the soluble enzymes of oxidative metabolism as well as substrates, nucleotide cofactors, and inorganic ions. The matrix also contains the mitochondrial genetic machinery – DNA, RNA and ribosomes – that generates several mitochondrial proteins **(43)**.

4. Electron transport chain

The 12 electron pairs released during glucose oxidation are not transferred directly to O_2. Rather, they are transferred to the coenzymes NAD^+ and FAD to form 10 NADPH and 2 $FADH_2$ (Figure 4) in the reactions catalyzed by the glycolytic enzyme,

pyruvate dehydrogenase and citric acid cycle enzymes. The electrons then pass into the mitochondrial electron-transport chain, a system of linked electron carriers.

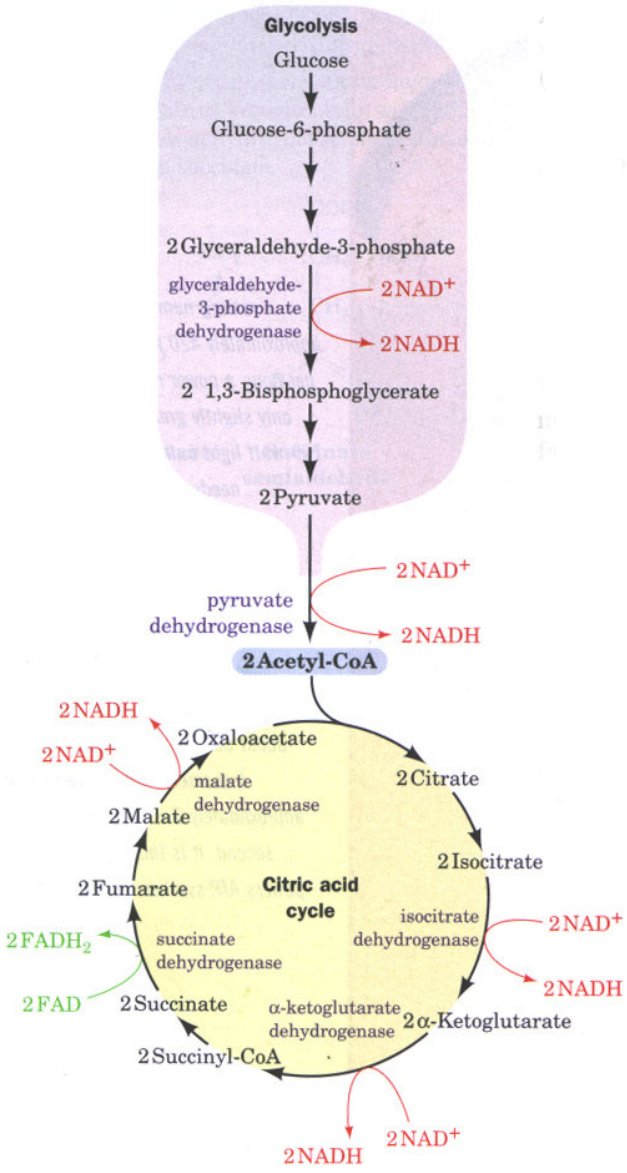

Figure 4 Site of electron transfer that form NADH and $FADH_2$ in glycolysis and the citric acid cycle **(43)**

The electron carriers that ferry electrons from NADH and $FADH_2$ to O_2 are associated with the inner mitochondrial membrane. Some of this redox centers are mobile, and others are components of integral membrane protein complexes.

Oxidation of NADPH and $FADH_2$ is carried out by the electron-transport chain, a set of protein complexes containing redox centers with progressively greater affinities for electrons. Electrons are carried from Complex I and II to Complex III by coenzyme Q (CoQ or ubiquinone), and from Complex III to Complex IV by the peripheral membrane protein cytochrome c. The following events occur during the electron transport:

Complex I catalyzes oxidation of NADH by CoQ:

$$NADH + CoQ\ (oxidized) \rightarrow NAD^+ + CoQ\ (reduced)$$

Complex III catalyzes oxidation of CoQ (reduced) by cytochrome c:

$$CoQ\ (reduced) + 2\ cytochrome\ c\ (oxidixed) \rightarrow CoQ\ (oxidized) + 2\ cytochrome\ c\ (reduced)$$

Complex IV catalyzes oxidation of reduced cytochrome c by O_2, the terminal electron acceptor of the electron-transport process:

$$2\ cytochrome\ c\ (reduced) + \tfrac{1}{2}\ O_2 \rightarrow 2\ cytochrome\ c\ (oxidized) + H_2O$$

As an electron pair successively traverses Complex I, III and IV, sufficient free energy is released at each step to power the synthesis of an ATP molecule.

Complex II catalyzes the oxidation of $FADH_2$ by CoQ:

$$FADH_2 + CoQ\ (oxidized) \rightarrow FAD + CoQ\ (reduced)$$

This redox reaction does not release sufficient free energy to synthesize ATP; it functions only to inject the electrons from $FADH_2$ into the electron transport chain **(43)**.

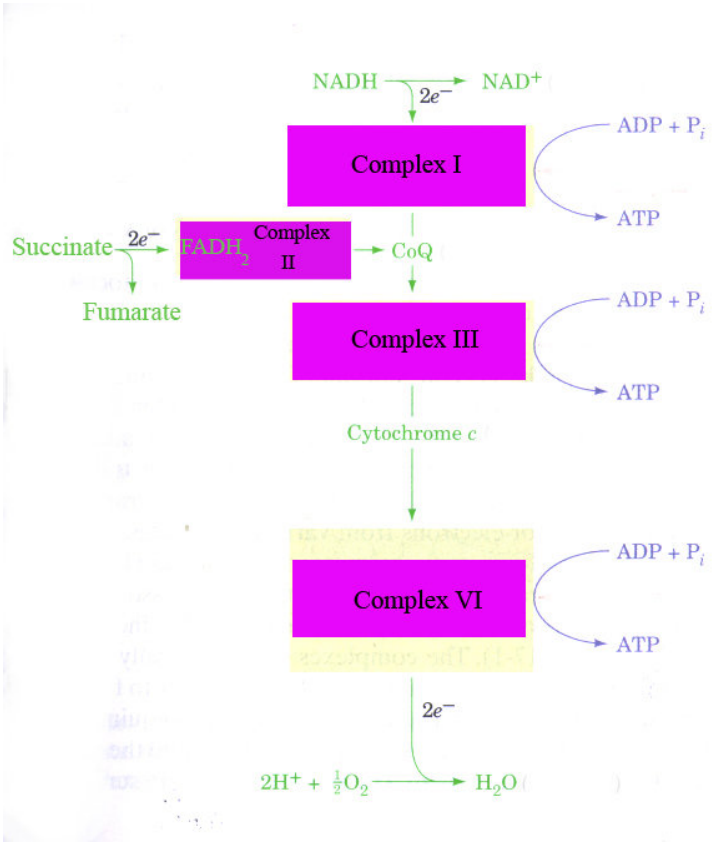

Figure 5 Electron Transport in mitochondrion

5. Reactive Oxygen Species (ROS)

Free radicals can be defined as molecules or molecular fragments containing one or more unpaired electrons in atomic or molecular orbitals **(44)**. This unpaired electron(s) usually gives a considerable degree of reactivity to the free radical. Radicals derived from oxygen represent the most important class of radical species generated in living systems. Molecular oxygen (dioxygen) has a unique electronic configuration and is itself a radical. The addition of one electron to dioxygen forms the superoxide anion radical ($O_2•^-$). Superoxide anion, arising either through metabolic processes or following oxygen "activation" by physical irradiation, is considered the "primary" ROS, and can further

interact with other molecules to generate “secondary” ROS, either directly or prevalently through enzyme- or metal-catalysed processes **(45)**.

The production of superoxide occurs mostly within the mitochondria of a cell. The mitochondrial electron transport chain is the main source of ATP in the mammalian cell and thus is essential for life. During energy transduction, a small number of electrons “leak” to oxygen prematurely, forming the oxygen free radical superoxide, which has been implicated in the pathophysiology of a variety of diseases **(46)**. Measurements on submitochondrial particles suggest an upper limit of 1–3% of all electrons in the transport chain “leaking” to generate superoxide instead of contributing to the reduction of oxygen to water **(45, 46)**. Superoxide is produced from both Complexe I and III of the electron transport chain, and once in its anionic form it is too strongly charged to readily cross the inner mitochondrial membrane **(47-49)**.

However, superoxide radical ion does not react directly with polypeptides, sugars, or nucleic acids, and its ability to peroxidise lipids is controversial. Superoxide is depleted undergoing a dismutation reaction (reaction (1)).

$$2O_2\bullet^- + 2H^+ \xrightarrow{SOD} H_2O_2 + O_2 \qquad (1)$$

Superoxide dismutase (SOD) enzymes accelerate this reaction in biological systems by about four orders of magnitude. It should be noted that SOD enzymes work in conjunction with H_2O_2- removing enzymes, such as catalases and glutathione peroxidases **(46)**.

The hydroxyl radical, •OH, is the neutral form of the hydroxide ion. The hydroxyl radical has a high reactivity, making it a very dangerous radical with a very short half-life. Thus when produced *in vivo* •OH reacts close to its site of formation. The redox state of the cell is largely linked to an iron (and copper) redox couple and is maintained within strict physiological limits. It has been suggested that iron regulation ensures that there is no free intracellular iron; however, *in vivo*, under stress conditions, an excess of superoxide releases “free iron” from iron-containing molecules. The release of iron by superoxide has been demonstrated for [4Fe–4S] cluster-containing enzymes of the

dehydratase-lyase family. The released Fe^{2+} can participate in the Fenton reaction (reaction (2)), generating highly reactive hydroxyl radical **(44, 45)**.

$$Fe^{2+} + H_2O_2 \rightarrow Fe^{3+} + \bullet OH + OH^- \qquad (2)$$

Thus under stress conditions, $O_2\bullet^-$ acts as an oxidant of [4Fe–4S] cluster-containing enzymes and facilitates •OH production from H_2O_2 by making Fe^{2+} available for the Fenton reaction. The superoxide radical participates in the Haber–Weiss reaction (reaction (3)) which combines a Fenton reaction and the reduction of Fe^{3+} by superoxide, yielding Fe^{2+} and oxygen (reaction (4)) **(45)**.

$$O_2\bullet^- + H_2O_2 \rightarrow O_2 + \bullet OH + OH^- \qquad (3)$$

$$Fe^{3+} + O_2\bullet^- \rightarrow Fe^{2+} + O_2 \qquad (4)$$

Additional reactive radicals derived from oxygen that can be formed in living systems are peroxyl radicals (ROO•). The simplest peroxyl radical is HOO•, which is the protonated form (conjugate acid; p*K*a ~4.8) of superoxide ($O_2\bullet^-$) and is usually termed either hydroperoxyl radical or perhydroxyl radical. Given this p*K*a value, only~0.3% of any superoxide present in the cytosol of a typical cell is in the protonated form. It has been demonstrated that hydroperoxyl radical initiates fatty acid peroxidation by two parallel pathways: fatty acid hydroperoxide (LOOH)-independent and LOOH-dependent. The LOOH-dependent pathway of $HO_2\bullet^-$ initiated fatty acid peroxidation may be relevant to mechanisms of lipid peroxidation initiation *in vivo*. Xanthine oxidase (XO) and xanthine dehydrogenase (XD) are interconvertible forms of the same enzyme, known as xanthine oxidoreductase (XOR). In purine catabolism, XOR catalyzes the oxidative hydroxylation of hypoxanthine to xanthine and subsequently of xanthine to uric acid. Uric acid acts as a potent antioxidant and free radical scavenger. XOR has, therefore, important functions as a cellular defense enzyme against oxidative stress. With both XO and XD forms, but particularly with the XO form, numerous ROS are synthesized. Thus, the synthesis of both an antioxidant (uric acid) and numerous free radicals makes XOR an important protective regulator of the cellular redox potential **(44)**.

Peroxisomes are known to produce H_2O_2, but not $O_2^{\bullet -}$, under physiologic conditions. Peroxisomes are major sites of oxygen consumption in the cell and participate in several metabolic functions that use oxygen. Oxygen consumption in the peroxisome leads to H_2O_2 production, which is then used to oxidize a variety of molecules. The organelle also contains catalase, which decomposes hydrogen peroxide and presumably prevents accumulation of this toxic compound. Thus, the peroxisome maintains a delicate balance with respect to the relative concentrations or activities of these enzymes to ensure no net production of ROS. How the organelle maintains this equilibrium is unclear. When peroxisomes are damaged and their H_2O_2 consuming enzymes downregulated, H_2O_2 releases into the cytosol which is significantly contributing to oxidative stress **(45)**.

6. Oxidative damage to DNA, lipids and proteins

At high concentrations, ROS can be important mediators of damage to cell structures, nucleic acids, lipids and proteins. The hydroxyl radical is known to react with all components of the DNA molecule, damaging both the purine and pyrimidine bases and also the deoxyribose backbone. The most extensively studied DNA lesion is the formation of 8-OH-G. Permanent modification of genetic material resulting from these “oxidative damage” incidents represents the first step involved in mutagenesis, carcinogenesis, and ageing **(45)**.

It is known that ROS results in an attack not only on DNA, but also on other cellular components involving polyunsaturated fatty acid residues of phospholipids, which are extremely sensitive to oxidation. Once formed, peroxyl radicals (ROO•) can be rearranged *via* a cyclisation reaction to endoperoxides (precursors of malondialdehyde) with the final product of the peroxidation process being malondialdehyde (MDA). The major aldehyde product of lipid peroxidation other than malondialdehyde is 4-hydroxy-2-nonenal (4-HNE) **(1, 2)**. MDA is mutagenic in bacterial and mammalian cells and carcinogenic in rats **(50)**. 4-HNE is weakly mutagenic but appears to be the major toxic product of lipid peroxidation **(1, 2, 51)**.

Mechanisms involved in the oxidation of proteins by ROS were elucidated by studies in which amino acids, simple peptides and proteins were exposed to ionizing radiations under conditions where hydroxyl radicals or a mixture of hydroxyl/superoxide radicals are formed. The side chains of all amino acid residues of proteins, in particular cysteine and methionine residues of proteins are susceptible to oxidation by the action of ROS. Oxidation of cysteine residues may lead to the reversible formation of mixed disulphides between protein thiol groups (–SH) and low molecular weight thiols, in particular GSH (*S*-glutathiolation). The concentration of carbonyl groups, generated by many different mechanisms is a good measure of ROS-mediated protein oxidation **(52)**

7. Lipid peroxidation

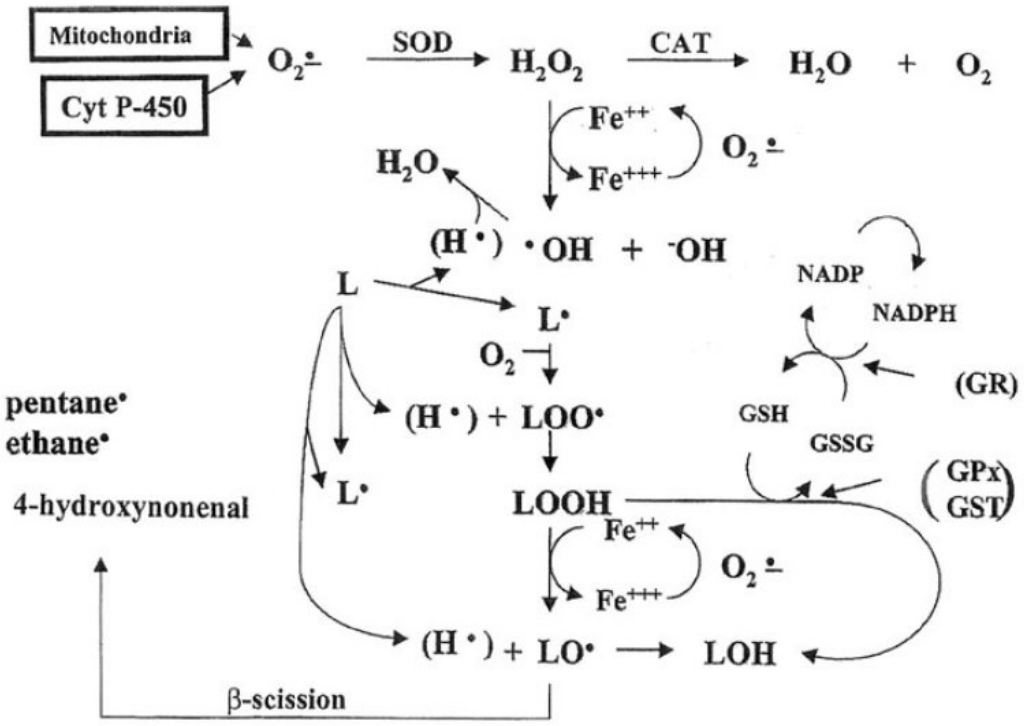

Figure 6 Lipid peroxidation process **(2)**

The polyunsaturated fatty acids in cholesterol esters, phospholipids, and triglycerides are subject to free radical-initiated oxidation and can participate in chain

reactions that amplify damage to biomolecules. Abstraction of a hydrogen atom from the polyunsaturated fatty acid (PUFA) moiety of membrane phospholipids initiates the process of lipid peroxidation (Figure 6). The resulting alkyl radical may rearrange to a more stable conjugated diene, which enters the autocatalytic lipid peroxidation cascade. Phospholipid hydroperoxides (PL-OOH) and fatty acid hydroperoxides (FA-OOH) constitute the major portion of the lipid peroxidation products and can propagate lipid peroxidation chain reactions. The fatty acid carbon chain may also be spontaneously cleaved (β-scission) during lipid peroxidation, yielding a variety of highly reactive compounds, including pentane and ethane radicals, and the α,β-unsaturated aldehydes. In particular 4-HNE, the major α,β –unsaturated aldehyde formed by the degradation of both ω-3 and ω-6 PUFA during lipid peroxidation is fairly stable and present in relatively higher amounts in biological membranes under the conditions of oxidative stress **(2, 51)**.

8. Defense against intracellular lipid peroxidation

In mammalian cells, there are two tiers of antioxidant defense mechanisms against ROS mediated lipid peroxidation. Low molecular mass compounds which act primarily against peroxyl radicals involved in radical propagation provide first line of defense against lipid peroxidation. These compounds referred as “chain-breaking antioxidants (CBAs)” can terminate the propagation of free radical mediated reactions and interrupt the autocatalytic chain reaction of lipid peroxidation. The main cellular CBAs include α-tocopherol, ascorbic acid, glutathione (GSH), uric acid, carotenoids, ubiquinone, and polyphenols, etc. Among these, GSH is particularly important because it also serves as the substrate for the two major antioxidant enzyme systems, glutathione peroxidases (GPxs) and glutathione *S* –transferases (GSTs). The antioxidant enzymes constitute the second line of defenses which provide a variety of primary and secondary defenses against oxidative stress. Primary antioxidant enzymes are mainly preventive and these enzymes such as superoxide dismuatase, catalase, and GPxs can decompose ROS and prevent the damage to cellular constituents and initiation of lipid peroxidation. Secondary defenses typically involve excision or repair of any lesions caused by ROS. In the event of ROS induced lipid peroxidation, secondary defense enzymes are involved in the

removal of LOOH to terminate the autocatalytic chain of lipid peroxidation and protect membranes. GPxs and GSTs which catalyze GSH-dependent reduction of LOOH (PL-OOH and FA-OOH) through their peroxidase activity are the major secondary defenses to guard against ROS-induced lipid peroxidation **(2)**.

9. 4-Hydroxy-2-nonenal (4-HNE)

9.1 Formation of 4-HNE

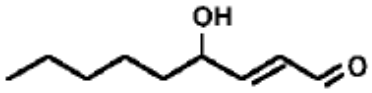

Figure 7 Structure of 4-hydroxy-2-nonenal

The mechanism of the formation of 4-HNE (Figure 7) has been a matter of debate since it was discovered as a major cytotoxic product of lipid peroxidation. It has been established that linoleic acid and arachidonic acid are among the potential precursors for 4-HNE formation, and that the nine carbons of 4-HNE are represented by the last nine carbons of these ω-6 essential fatty acids. In 1993, Gardner and Hamberg demonstrated the first experimental evidence for a pathway from fatty acid hydroperoxides to 4-HNE, in which they established that the aldehydic product of the reaction of 9-hydroperoxylinoleic acid with hydroperoxide lyase, namely 3*Z*-nonenal, can be converted to 4-hydroperoxy-2*E*-nonenal (4-HPNE) by a reaction with molecular oxygen, mainly catalyzed in this case by a 3*Z*-alkenal oxygenase **(53)**. In addition, they also substantiated an additional route to 4-HNE *via* peroxygenase reactions utilizing the co-substrates 3*Z*-nonenal and 4-HPNE; the existence of a nonenzymatic pathway was also implicated **(53)**. Subsequent work by Gardner and Grove (1998) showed that 3*Z*-nonenal is a substrate for soybean lipoxygenase, which thus could function as a 3*Z*-alkenal oxygenase and that the product is 4-HPNE **(54)**. More recently, in an elegant study using the 9- and 13-hydroperoxides of linoleic acid as starting materials, Brash and his colleagues found that two distinct mechanisms lead to the formation of 4-HPNE, in which allylic hydrogen abstraction at C-8 of 13*S*-hydroperoxy-9*Z*,11*E*-octadecadienoic

acid (13*S*-HPODE) leads to a 10,13-dihydroperoxide that undergoes cleavage between C-9 and C-10 to give 4*S*-HPNE, whereas 9*S*-HPODE cleaves directly to 3*Z*-nonenal as a precursor of racemic 4-HPNE **(55)**. 4-HPNE may be subsequently converted to 4-HNE and 4-oxo-2*E*-nonenal (ONE).

9.2 Metabolism of 4-HNE

Mammalian cells have developed multiple enzymatic pathways for the detoxification of 4-HNE. The best characterized of these enzymes include the glutathione *S*-transferases (GSTs), aldehyde dehydrogenase, and alcohol dehydrogenase **(1)**. GSTs catalyze conjugation of GSH to 4-HNE *via* Michael addition at the C-3 carbon, thereby preventing further nucleophilic addition to this toxic compound **(5, 56)**. Aldehyde dehydrogenase catalyzes the oxidation of 4-HNE to the innocuous 4-hydroxy-2-nonenoic acid, while alcohol dehydrogenase catalyzes reduction of the terminal aldehyde to its alcohol, yielding the unreactive metabolite 1,4-dihydroxy-2-nonene. Other than these main enzymes involved in the metabolism of 4-HNE, aldose reductase, a member of the aldoketo reductase superfamily, has been reported to contribute to the metabolism of 4-HNE. The enzyme has also been shown to catalyze the reduction of the glutathione conjugate of 4-HNE **(1, 51)**.

10. Pathological effects of 4-HNE

10.1 Atherosclerosis

It has been proposed that LDL, the key component of the fatty streak lesion of atherosclerosis, must undergo oxidative modification before it can give rise to foam cells **(4)**. Indeed, Palinski, W., et al. (1990) showed that 4-HNE-lysine adducts develop on apo-lipoprotein B during copper-induced oxidation of LDL *in vitro* by using the antiserum and monoclonal antibody which specific for 4-HNE-lysine. Viera, O. et al. (2000) also showed that oxidized LDL induced derivatization of cell proteins by 4-HNE and ubiquination in ECV-304, human endothelial cell line. They purposed that this event

might be involved in the mechanism of oxidized LDL-induce apoptosis **(57)**. Moreover, the presence of 4-HNE adducts immunoreactive to the antibody against the 4-HNE-lysine fluorophore was also confirmed in the atherosclerotic lesions of human aorta **(3)**.

10.2 Cancer

4-HNE is able to react readily with various cellular components, including proteins and DNA. It has been found that 4-HNE can interact with DNA to form 4-HNE-dG adduct, which is a strong mutagen and induces mainly Guanine:Cytosine to Thymine:Adenine mutations in human cells. Moreover, 4-HNE-dG adduct preferentially form at codon 249 of the p53 gene, a mutational hotspot in human cells **(7)**. Feng, Z., et al. (2004) found that 4-HNE can greatly inhibit nucleotide excision repair of DNA damage induced by benzo[*a*]pyrene diol epoxide, a major carcinogen in cigarette smoke and environment, as well as damage induced by ultraviolet light irradiation in both human colon and lung epithelial cells. The effect of 4-HNE on DNA repair was further confirmed by its inhibitory effect on DNA repair in an *in vitro* DNA repair synthesis system, and this effect is mainly caused by the direct modification of repair proteins by 4-HNE. They have also found that 4-HNE can greatly enhance the sensitivity of human cells to benzo[*a*]pyrene diol epoxide and ultraviolet-induced cell killing. Together, these results strongly suggest that 4-HNE damages not only DNA but also DNA repair mechanisms. Due to these two detrimental effects, 4-HNE may contribute synergistically to human carcinogenesis **(7)**.

10.3 Chronic Obstructive Pulmonary Disease (COPD)

Using a mouse monoclonal antibody against 4-HNE adduct in immunohistochemistry, Rahman and his colleagues (2002) assessed the relations between 4-HNE-modified protein levels, force expiratory in 1 second (FEV_1), γ-glutamylcysteine synthetase (γ-GCS), transforming growth factor-β_1 (TGF-β_1). 4-HNE modified protein levels were elevated in airway and alveolar epithelial cells, endothelial cells, and

neutrophils in subjects with COPD, compared with the levels in subjects without COPD. Moreover, they also observed a significant inverse correlation between the levels of 4-HNE adducts in alveolar epithelium, airway endothelium, and neutrophils and FEV_1 and positive correlation between 4-HNE adducts and TGF-β_1 protein and γ-GCS mRNA in airway and alveolar epithelium **(8)**. The 4-HNE modified proteins have also been detected in COPD patients' alveolar macrophages **(11)**. The elevated levels of 4-HNE may play a role in the signaling events in lung inflammation leading to imbalance of expression of both proinflammatory mediators and protective antioxidant genes in COPD **(8)**.

10.4 Neurodegenerative diseases

The presence of 4-HNE-derived epitopes, including 4-HNE Michael and pyrrole adducts, has been reported in the most common neurodegenerative diseases, such as Alzheimer's disease **(23)**, Parkinson's disease **(14)**. These findings provide support for the involvement of oxidative stress (lipid peroxidation) in the pathogenesis of neurodegenerative diseases. The exact role of 4-HNE in neurodegenerative disorders has yet as to be established, but it is acknowledged that 4-HNE is a highly toxic compound capable of causing neuronal cell death **(17, 58)**.

11. 4-HNE induced apoptosis

Apoptosis, a mode of cell death, plays a crucial role normal cell turnover, proper development and functioning of the immune system, hormone-dependent atrophy, embryonic development and chemical-induced cell death as a physiological event, regulating cell number and eliminating damaged cells. Apoptosis is the most common form of eukaryotic cell death. It is a physiological suicide mechanism that preserves homeostasis, in which cell death naturally occurs during tissue turnover. In general, cells undergoing apoptosis display profound structural changes, including a rapid blebbing of the plasma membrane and nuclear disintegration. The nuclear collapse is associated with extensive damage to chromatin and DNA cleavage **(59)**.

4-HNE has been suggested to be a potential inducer of apoptotic cell death. The apoptosis-inducing activity of 4-HNE appears in a dose and time dependent manner in various cells **(17, 28, 60, 61)**. The intracellular events, c-Jun N-terminal protein kinase (JNK) activation **(26, 62, 63)** , GSH depletion **(56)**, and activation of a Fas-independent caspase cascade **(64)**, have been suggested to be involved in the major apoptotic pathway initiated by 4-HNE. Ji, C., et al. (2001) have investigated the mechanism of 4-HNE induced cell death in RKO cells, human colorectal carcinoma cells, and demonstrated that 4-HNE induces apoptosis by inducing alteration of mitochondrial function leading to release of cytochrome c and subsequent activation of the caspase cascade **(65)**.

12. 4-HNE induced ROS generation

There is increasing evidence that 4-HNE generated endogenously during the process of lipid peroxidation is causally involved in most of the pathophysiological effects associated with oxidative stress in cells and tissues. Compared with free radicals, 4-HNE is generally stable and can diffuse within or even escape from the cell and attack targets far from the site of the original free radical initiated event, therefore suggesting that it is not only end products and remnants of lipid peroxidation processes but also may act as mediators for the primary free radicals that initiated lipid peroxidation **(1)**.

It has been suggested that 4-HNE provides a link between oxidant generation, lipid peroxidation, and cell death. 4-HNE produced with relatively large amounts is believed to be responsible for oxidative stress induced cell death. Moreover, an increasing number of evidences indicate that 4-HNE-induced cytotoxicity through an increased intracellular ROS production in various cells **(24-27)**. Recently, Lee, J.Y., et al. (2006) found that mitochondrial dysfunction plays a key role in mediating 4-HNE induced vascular smooth muscle cell apoptosis through an increased mitochondrial production of ROS **(28)**

CHAPTER III
MATERIALS AND METHODS

Materials

The human bladder carcinoma cell line ECV-304 was obtained from American Type Culture Collection (Rockville, MD). Dulbecco's modified Eagle's medium (DMEM), fetal bovine serum (FBS) and penicillin/streptomycin were purchased from Gibco (NY, USA). Dichlorodihydrofluorescein diacetate ($DCFH_2$-DA) and Hoechst 33342 were obtained from Invitrogen (CA, USA). 3-(4,5-dimethylthiazol-2-yl)-2,5-diphenyltetrazolium bromide (MTT), propidium iodide (PI), N-acetyl-L-cysteine (NAC) and glutathione (GSH) were purchased from Sigma-Aldrich (St.Louis, MO, USA). 4-hydroxy-2-nonenal (4-HNE) was obtained from Cayman Chemical Company (Ann Arbor, MI). Asiaticoside (Batch no AS0303610) was purchased from Changzhou Natural Products (Development Co, Ltd, China).

Methods

1. Cell culture

The ECV-304 cells were cultured in DMEM containing 10% FBS, 100 units/ml penicillin/streptomycin in a 5% CO_2 environment at 37°C.

2. Cell viability assay

Cell viability was determined by MTT assay. MTT (3-(4, 5-dimethylthiazol-2-y1)-2,5-diphenyltetrazolium bromide) is a yellow water-soluble tetrazolium salt. The dye is converted to water-insoluble purple formazan on the reductive cleavage of its tetrazolium ring by the succinate dehydrogenase system of the active mitochondria. Hence, the amount of formazan formed can be determined spectrophotometrically and

serves as an estimate of the number of mitochondria and hence the number of living cells in the sample **(66)**.

Cells were seeded at a density 2 x 10^3 cells/well in a 96-well plate and treated as described in 2.1, 2.2 and 2.3. After treatment, the cells were incubated with MTT (final concentration 1 mM) for 4 hours at 37°C and then added 100 µl of DMSO to solubilize formazan crystals. Cell viability was determined by using a microplate reader (Biorad, model 3550) at 570 nm (630 reference filter). The cellular reduction of MTT, which reflects metabolic activity and viability, was expressed in term of relative cell viability as compared to that in untreated control.

2.1 Effect of 4-HNE on ECV-304 cells

To examine the role of 4-HNE on ECV-304 cells, subconfluent (90%) monolayers of ECV-304 cells were incubated with various concentrations of 4-HNE (0, 5, 10, 20 and 40 µM) and cell viability was evaluated after 24 hours by MTT assay.

2.2 Effect of asiaticoside on ECV-304 cells

To investigate whether asiaticoside has cytotoxic effect to ECV-304 cells, subconfluent (90%) monolayers of ECV-304 cells were treated with various concentrations of asiaticoside (0, 5, 10, 100 and 200 µM) and viable cells were determined after 24 hours by MTT assay.

2.3 Effect of antioxidants on 4-HNE induced cytotoxicity

To determine the role of antioxidants on 4-HNE induced cytotoxicity, subconfluent (90%) monolayers of ECV-304 cells were co-treated with antioxidants, NAC (1 mM) or GSH (1 mM), and 20 µM of 4-HNE and cell viability was analyzed after 24 hours by MTT assay.

2.4 Effect of asiaticoside on 4-HNE induced cytotoxicity

To investigate the role asiaticoside on 4-HNE induced cytotoxicity, subconfluent (90%) monolayers of ECV-304 cells were co-treated with various concentrations of asiaticoside (0, 5, 10, 100 and 200 μM) and 20 μM of 4-HNE and cell viability was measured after 24 hours using MTT assay.

3. Measurement of apoptotic and necrotic cells

Apoptosis was determined by using Hoechst 33342 dye. Hoechst 33342 is a noncytotoxic DNA dye that preferentially binds to triplet adenine and thymine base pairs in the minor groove outside of the double helix. Nuclear morphological changes of apoptotic cells were assessed by using the fluorescent dye Hoechst 33342 **(67)**.

Propidium iodide (PI) is a nucleic acid stain usually used as a counterstain in multicolor fluorescent techniques. Since PI is membrane impermeant, it is also used to detect necrotic cells in culture. When the cell membrane is disrupted, it leaks into the cell and binds to DNA and RNA and, therefore, only necrotic cells fluoresce red **(68)**.

Cells were seeded at a density 2 x 10^3 cells/well onto 96-well plate and treated as described in 3.1, 3.2 and 3.3. After treatment, the cells were stained with Hoechst 33342 (final concentration 10 μM) and PI (final concentration 10 μM) for 30 minutes in dark. Fluorescence images were recorded using fluorescence microscope (model IX51, Olympus, Tokyo, Japan). Images were acquired using a 40x objective. The apoptotic cells were expressed in term of the percentage of cells having intensely condensed chromatin and/or fragmented nuclei. The necrotic cells were expressed in term of the percentage of cells fluorescing red. At least three replicate wells were analyzed for each treatment of five random fields in each well.

3.1 Determining apoptotic and necrotic changes of 4-HNE

To evaluate the role of 4-HNE, subconfluent (90%) monolayers of ECV-304 cells were treated with various concentrations of 4-HNE (0, 5, 10, 20 and 40 μM) and cell death was determined after 12 hours by using Hoechst 33342 and PI staining.

3.2 Determining apoptotic and necrotic changes of asiaticoside

To examine whether asiaticoside could induce cell death, subconfluent (90%) monolayers of ECV-304 cells were treated with various concentrations of asiaticoside (0, 5, 10, 100 and 200 μM) for 12 hours and then death mechanism was analyzed by using Hoechst 33342 and PI staining.

3.3 Effect of antioxidants on 4-HNE induced apoptosis and necrosis

To determine the role of antioxidants on 4-HNE induced cell death, subconfluent (90%) monolayers of ECV-304 cells were co-treated with antioxidants, NAC (1 mM) or GSH (1 mM), and 4-HNE (20 μM) and cell death was evaluated after 12 hours by using Hoechst 33342 and PI staining.

3.4 Effect of asiaticoside on 4-HNE induced apoptosis and necrosis

To investigate the role of asiaticoside on 4-HNE induced cell death, subconfluent (90%) monolayers of ECV-304 cells were co-treated with various concentrations of asiaticoside (0, 5, 10, 100, 200 μM) and 4-HNE (20 μM) for 12 hours and then death mechanism was determined by using Hoechst 33342 and PI staining.

4. Assay of ROS formation

Intracellular ROS formation was measured by fluorescence using 2',7' – dichlorodihydrofluorecein diacetate ($DCFH_2$-DA), a dye that permeates cells where it is

trapped as the deesterified free acid, which can react with ROS to form a highly fluorescent 2',7' – dichlorofluorecein (DCF) **(27)**.

Cells were resuspended in ice cold PBS at a density 5 x 10^4 cells/ml and incubated with $DCFH_2$-DA at a final concentration of 5 μM for 30 minutes. Then, cells were washed twice with ice cold PBS to remove extracellular $DCFH_2$-DA and resuspended in PBS. Different agents, which described in 4.1, 4.2 and 4.3, were added in each samples at 37°C. The fluorescence was immediately analyzed by flow cytometry using a 488 nm excitation beam and a 538 nm band-pass filter (FACSort, Becton Dickinson, Rutherford, NJ) with CellQuest software (Becton Dickinson). The DCF fluorescence intensity, which reflects intracellular ROS level, was expressed in term of relative DCF fluorescence as compared to that in untreated control.

4.1 Effect of 4-HNE on intracellular ROS formation in ECV-304 cells

Intracellular ROS level was determined in the function of time and dose. For time dependent study, subconfluent (90%) monolayers of ECV-304 cells were incubated with 20 μM of 4-HNE at various incubation times (0, 30, 60 and 120 minutes) in serum-free medium. At each time point, the intracellular ROS level was determined using flow cytometer and $DCFH_2$-DA as described.

For concentration dependent study, subconfluent (90%) monolayers of ECV-304 cells were treated with various concentrations of 4-HNE (0, 5, 10, 20 and 40 μM) for 120 minutes in serum-free medium. Then, the intracellular ROS level was determined using flow cytometer and $DCFH_2$-DA as described.

4.2 Effect of antioxidants on 4-HNE induced intracellular ROS formation in ECV-304 cells

To investigate the role of antioxidants on 4-HNE induced intracellular ROS generation, subconfluent (90%) monolayers of ECV-304 cells were co-treated with antioxidants, NAC (1 mM) or GSH (1mM), and 4-HNE (20 μM) for 120 minutes and

intracellular ROS level was measured by using flow cytometer and $DCFH_2$-DA as described.

4.3 Effect of asiaticoside on 4-HNE induced intracellular ROS formation in ECV-304 cells

To examine the role of asiaticoside on 4-HNE induced intracellular ROS formation, subconfluent (90%) monolayers of ECV-304 cells were co-treated with asiaticoside (0, 5, 10, 100 and 200 μM) and 4-HNE (20 μM) and intracellular ROS level was measured after 120 minutes by using flow cytometer and $DCFH_2$-DA as described.

5. Analysis of the intracellular ROS level

Intracellular ROS formation was determined by fluorescence using 2',7' – dichlorodihydrofluorecein diacetate ($DCFH_2$-DA), a dye that permeates cells where it is trapped as the deesterified free acid, which can react with ROS to form a highly fluorescent 2',7' – dichlorofluorecein (DCF) **(27)**. Intracellular DCF fluorescence was visualized by fluorescence microscopy.

Cells were seeded at a density 2 x 10^3 cells/wel onto 96-well plate and incubated with $DCFH_2$-DA at a final concentration of 5 μM for 30 minutes. After 30 minutes, different agents, which described in 3.1, 3.2, 3.3 and 3.4, were added in each samples at 37 °C. Fluorescence images were recorded using fluorescence microscope (model IX51, Olympus, Tokyo, Japan). Images were acquired using a 10x objective. At least three replicate wells were analyzed for each treatment of five random fields in each well.

5.1 Effect of 4-HNE on intracellular ROS formation in ECV-304 cells

Intracellular ROS level was determined in the function of time and dose. For time dependent study, subconfluent (90%) monolayers of ECV-304 cells were treated with 20 μM of 4-HNE at various incubation times (0, 30, 60 and 120 minutes) in serum-

free medium. At each time point, the intracellular ROS level was visualized by fluorescence microscopy as described.

For concentration dependent study, subconfluent (90%) monolayers of ECV-304 cells were treated with various concentrations of 4-HNE (0, 5, 10, 20 and 40 μM) for 120 minutes in serum-free medium. Then, the intracellular ROS level was visualized by fluorescence microscopy as described.

5.2 Effect of antioxidants on 4-HNE induced intracellular ROS formation in ECV-304 cells

To determine the role of antioxidants on 4-HNE induced intracellular ROS generation, subconfluent (90%) monolayers of ECV-304 cells were co-treated with antioxidants, NAC (1 mM) or GSH (1mM), and 4-HNE (20 μM) and the intracellular ROS level was visualized after 120 minutes by fluorescence microscopy as described.

5.3 Effect of asiaticoside on 4-HNE induced intracellular ROS formation in ECV-304 cells

To investigate the role of asiaticoside on 4-HNE induced intracellular ROS generation, subconfluent (90%) monolayers of ECV-304 cells were co-treated with various concentrations of asiaticoside (0, 5, 10, 100 and 200 μM) and 4-HNE (20 μM) and the intracellular ROS level was visualized after 120 minutes by fluorescence microscopy as described.

6. Statistics

Data were expressed as means ± standard error of mean (S.E.M.). The reproducibility of the results was confirmed at least three independent sets of experiments. Data shown in figures were from a representative set of experiments. All data represent at least three independent experiments and were expressed as the mean ± S.E.M. unless otherwise indicated. Differences between groups were analyzed using one

way analysis of variance (ANOVA) followed by Tukey's test for multiple comparisons. Groups were considered to show statistically significant difference if the *P*-value was less than 0.05. All statistic data were analyzed by SPSS Statistics Base 17.0 (Network license which purchased by Chulalongkorn University).

7. Experimental Design

The methods were designed as the following. Cell viability was detected by using MTT assay. Death mechanism was analyzed by fluorescence microscopic assay staining with Hoechst 33342 and PI. Intracellular ROS formation was visualized by fluorescence microscopic assay staining with $DCFH_2$-DA and measured by flow cytometric analysis using $DCFH_2$-DA.

The study was divided into 5 parts as follows:

1. Determining cytotoxic effect of 4-HNE on ECV-304 cells
2. Determining cytotoxic effect of asiaticoside on ECV-304 cells
3. Determining effect of 4-HNE on intracellular ROS formation in ECV-304 cells
4. Determining effect of asiaticoside on 4-HNE induced cell death in ECV-304 cells
5. Determining effect of asiaticoside on 4-HNE induced intracellular ROS formation in ECV-304 cells

CHAPTER IV
RESULTS

1. Cell viability assay

The effect of substance on cell viability was determined in ECV-304 cells by using MTT assay, in which the mitochondrial dehydrogenase function in viable cells was detected.

1.1 Effect of 4-HNE on ECV-304 cell survival.

To investigate the role of 4-HNE on cell viability, ECV-304 cells were treated with various concentrations of 4-HNE (0-40 μM) and cell viability was determined after 24 hours by MTT assay. As shown in Figure 8, low concentrations of 4-HNE (0-10 μM) did not cause significant toxicity ($P > 0.05$) on ECV-304 cells. High concentrations of 4-HNE, 20 μM and 40 μM, caused a concentration-dependent decrease in cell viability with approximately 0.61 and 0.28 of the remained viable cells.

1.2 Effect of asiaticoside on ECV-304 cell survival.

To investigate whether asiaticoside has an effect on ECV-304 cell viability, cells were treated with various concentrations of asiaticoside (0-800 μM) and cell viability was determined after 24 hours by MTT assay. The results indicated that asiaticoside at concentrations ranging from 0-200 μM did not show significant toxicity ($P > 0.05$) on ECV-304 cell survival (Figure 9), while asiaticoside at the concentrations of 400 μM and 800 μM significantly reduced ($P < 0.05$) relative cell viability to 0.26 ± 0.02 and 0.02 ± 0.00, respectively.

1.3 Effect of antioxidants on 4-HNE induced cytotoxicity

To provide supporting evidence for the involvement of ROS in the 4-HNE cytotoxicity, ECV-304 cells were incubated with the toxic concentration of 4-HNE (20 μM) in the presence or absence of antioxidants (NAC 1 mM or GSH 1 mM) and analyzed for cell survival by MTT assay. 4-HNE at the concentration of 20 μM significantly decreased ($P < 0.05$) relative cell viability to 0.41 ± 0.02. Addition of NAC or GSH significantly attenuated ($P < 0.05$) the toxic effect of 4-HNE with cell viability back to 0.91 ± 0.01 and 0.85 ± 0.01, respectively, which was nearly equal to the untreated control (1.00 ± 0) (Figure 10).

1.4 Effect of asiaticoside on 4-HNE induced cytotoxicity

To investigate whether asiaticoside could inhibit toxic effect of 4-HNE in these cells, ECV-304 cells were treated with toxic concentration of 4-HNE (20 μM) in the presence or absence of asiaticoside (0-200 μM) and cell survival was determined after 24 hours using MTT assay. The addition of asiaticoside clearly protected ECV-304 cells from 4-HNE induced cell death. The relative cell viability of 20 μM 4-HNE treated cells was 0.34 ± 0.01, while addition of asiaticoside 5 μM, 10 μM, 100 μM, or 200 μM increased cell viability of ECV-304 to 0.61 ± 0.00, 0.61 ± 0.01, 0.74 ± 0.01 and 0.77 ± 0.01, respectively (Figure 11).

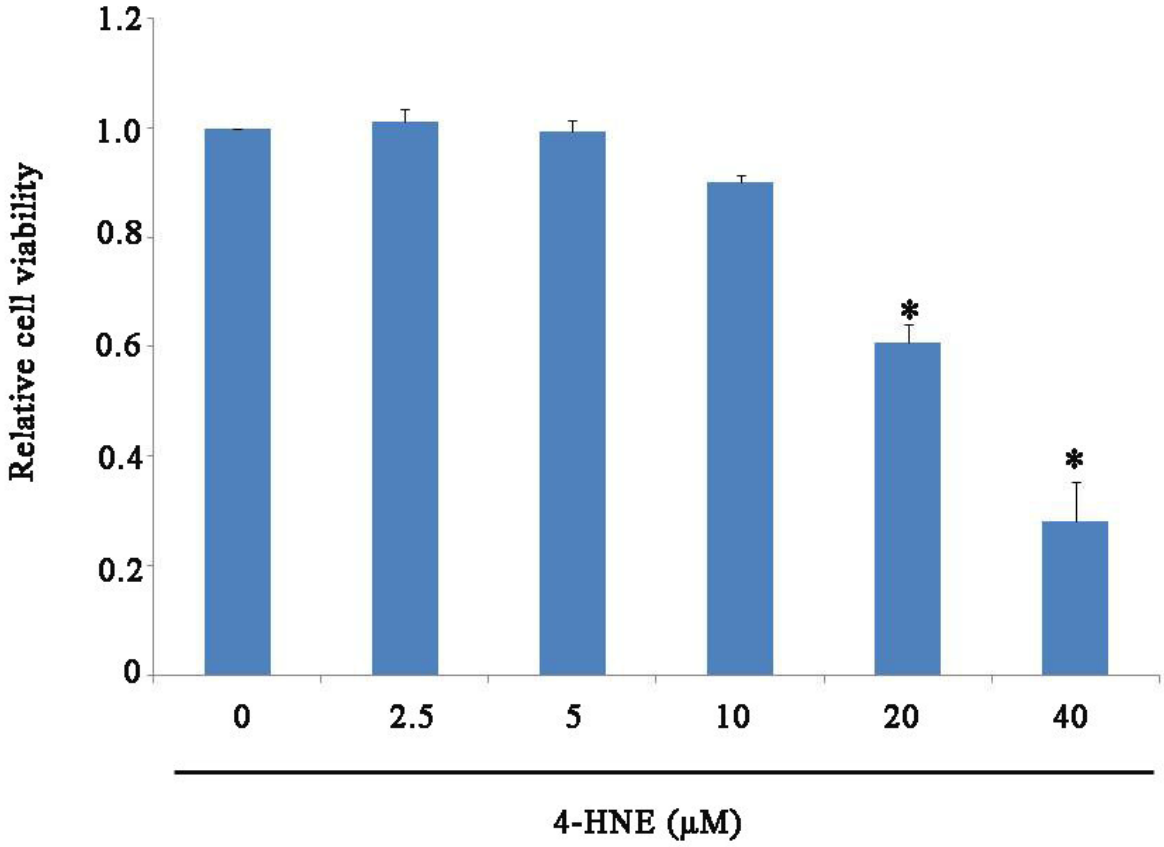

Figure 8 Effect of 4-HNE on cell viability. Cells were incubated with various concentrations of 4-HNE (0-40 μM) for 24 hours and the cell viability was measured by MTT assay. The results were expressed as mean ± S.E.M. of relative cell viability determined from three independent experiments. Statistical significance: * $P < 0.05$ versus untreated control analyzed by repeated measure ANOVA and Tukey's post test.

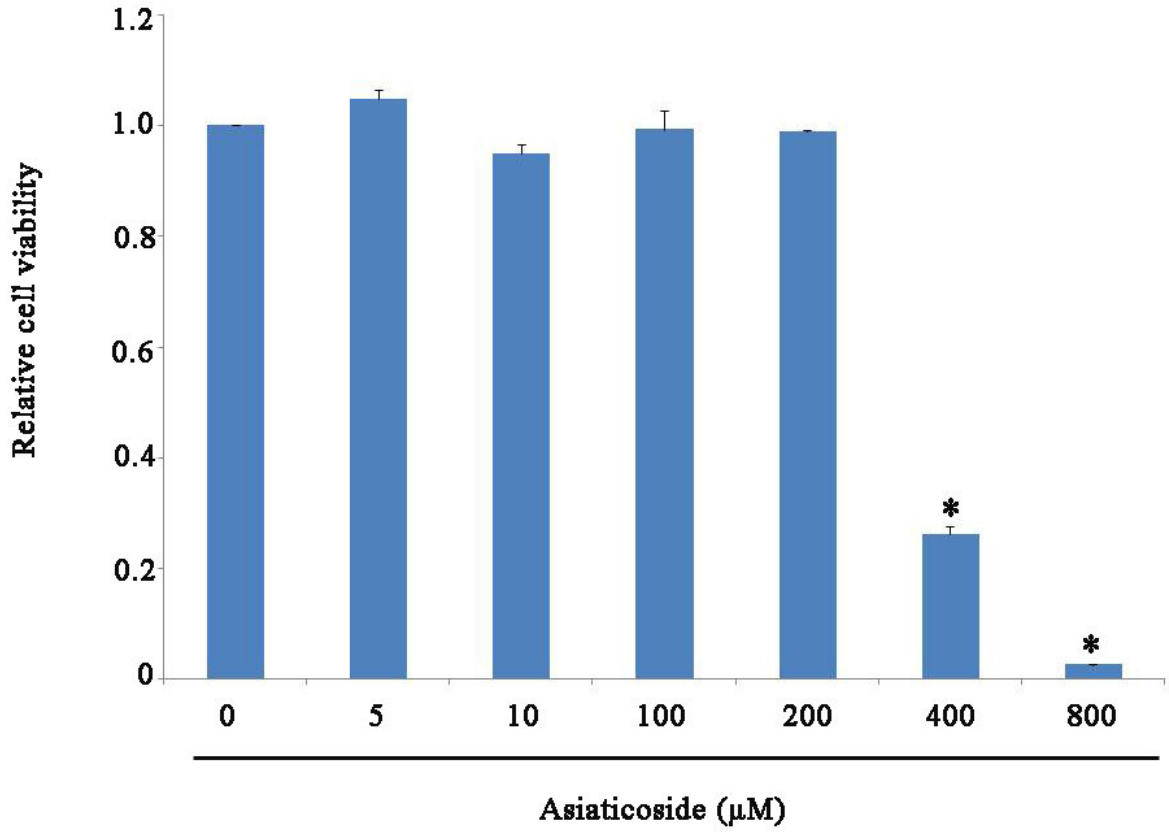

Figure 9 Effect of asiaticoside on cell viability. ECV-304 cells were incubated with various concentrations of asiaticoside (0-800 μM) for 24 hours and the cell viability was measured by MTT assay. The results were expressed as mean ± S.E.M. of relative cell viability determined from three independent experiments. Statistical significance: * $P < 0.05$ versus untreated control analyzed by repeated measure ANOVA and Tukey's post test.

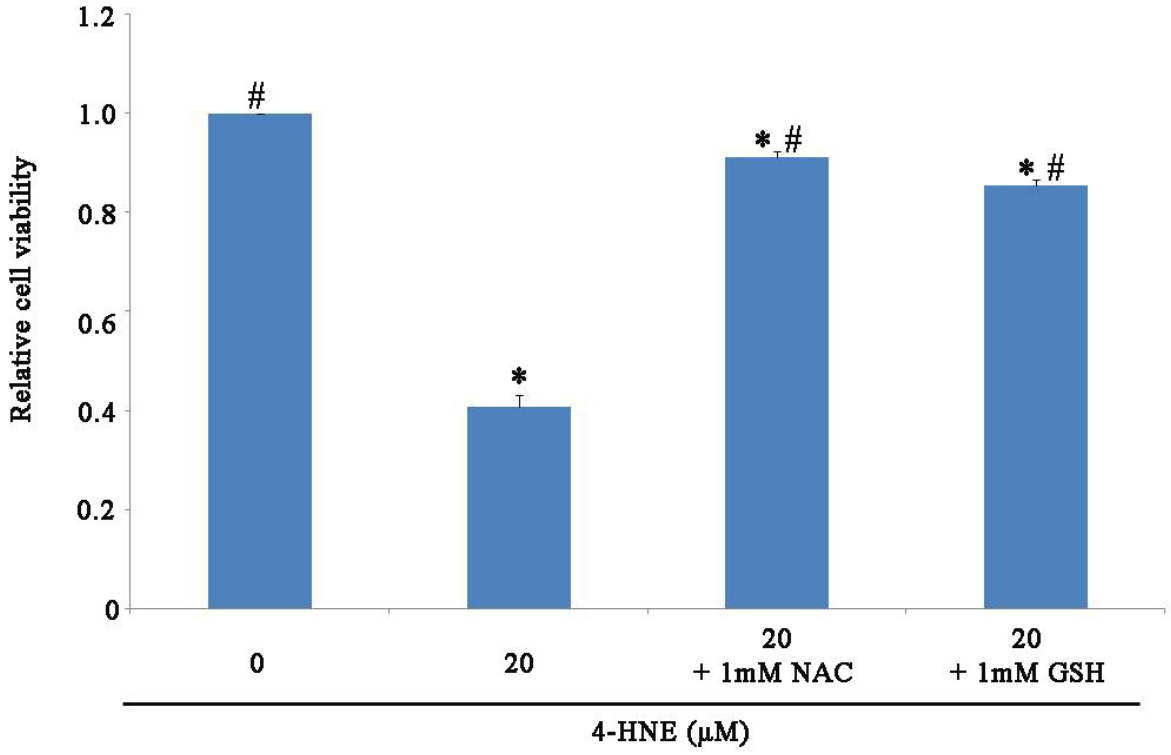

Figure 10 Effect of antioxidants on 4-HNE induced cytotoxicity. The cells were co-treated with antioxidant, NAC (1mM) or GSH (1mM), and 4-HNE (20 μM). After 24 hours, the cell viability was measured by MTT assay. The results were expressed as mean ± S.E.M. of relative cell viability determined from three independent experiments. Statistical significance: * $P < 0.05$ versus untreated control, # $P < 0.05$ versus 4-HNE (20 μM) treated group analyzed by repeated measure ANOVA and Tukey's post test.

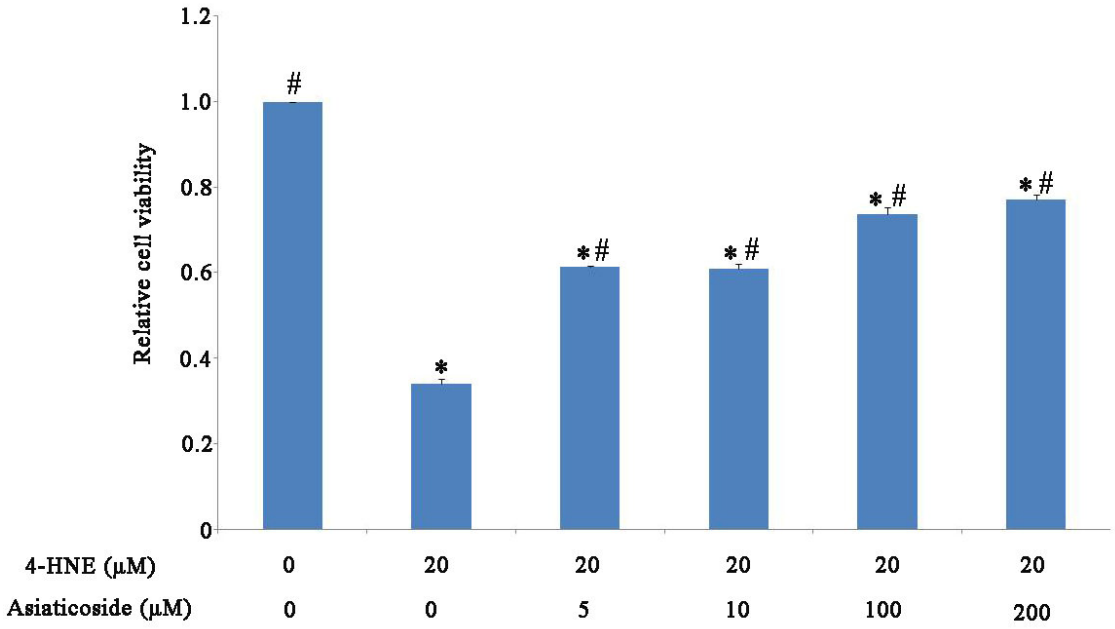

Figure 11 Effect of asiaticoside on 4-HNE induced cytotoxicity. The cells were co-treated with asiaticoside (0-200 μM) and 4-HNE (20 μM) for 24 hours. The cell viability was measured by MTT assay. The results were expressed as mean ± S.E.M. of relative cell viability determined from three independent experiments. Statistical significance: * $P < 0.05$ versus untreated control, # $P < 0.05$ versus 4-HNE (20 μM) treated group analyzed by repeated measure ANOVA and Tukey's post test.

2. Detection of apoptosis and necrosis

The cell death mechanisms, apoptosis or necrosis, by which substance-induced cytotoxicity was characterized using Hoechst 33342 and PI staining assay.

2.1 4-HNE induced apoptosis and necrosis

To investigate cell death mechanisms in response to 4-HNE induced cytotoxicity, ECV-304 cells were incubated with various concentrations of 4-HNE (0-40 μM) and cell death was evaluated after 12 hours using Hoechst 33342 and PI staining assay. Approximately 12% and 8% of the treated cells showed apoptotic and necrotic morphology after exposure with 20 μM 4-HNE, respectively (Figure 12B).

The nuclear morphological analysis of untreated control and 4-HNE treated cells were shown in Figure 12A.

2.2 Effect of antioxidants on 4-HNE induced cell death

To establish the correlation between 4-HNE induced cell death and ROS formation, ECV-304 cells were incubated with the toxic concentration of 4-HNE (20 μM) in the presence or absence of antioxidants (NAC 1 mM or GSH 1 mM) and analyzed for cell death by Hoechst 33342 and PI staining assay. Cell apoptosis was significantly increased (12.15 ± 1.09 %) ($P < 0.05$) in response to the treatment of 20 μM 4-HNE. Addition of NAC or GSH significantly attenuated ($P < 0.05$) 4-HNE effect with decreased apoptosis to 4.17 ± 0.62 and 3.82 ± 1.26, respectively. In case of necrosis, addition of NAC or GSH significantly decreased ($P < 0.05$) necrotic cells to 3.14 ± 1.24, 3.73 ± 1.08, as compared to the incubation with 4-HNE alone (7.79 ± 0.10%) (Figure 13B).

The nuclear morphological analysis of untreated control, 4-HNE treated cells and 4-HNE with antioxidant co-treated cells were shown in Figure 13A.

2.3 Effect of asiaticoside on 4-HNE induced cell death

To investigate whether asiaticoside could induce cell death, ECV-304 cells were incubated with various concentrations of asiaticoside (0-200 μM) and cell death was determined by using Hoechst 33342 and PI staining assay. Exposure with asiaticoside (0-200 μM) alone induced neither apoptosis nor necrosis in ECV-304 (Figure 14A, 14B).

To investigate whether asiaticoside could inhibit 4-HNE induced cell death, ECV-304 cells were treated with toxic concentration of 4-HNE (20 μM) in the presence or absence of asiaticoside (0-200 μM) and apoptosis and necrosis were evaluated after 12 hours incubation using Hoechst 33342 and PI staining assay. Addition of asiaticoside clearly protected ECV-304 cells from 4-HNE induced apoptosis. Importantly, 4-HNE at the concentration of 20 μM caused 12.15 ± 1.09 % cell apoptosis, which was significant decreased ($P < 0.05$) in response to 5 μM, 10 μM, 100 μM, and 200 μM of asiaticoside co-treatment with apoptotic cell death 5.88 ± 0.60 %, 5.74 ± 1.09 %, 6.17 ± 1.01 % and 6.19 ± 0.91 %, respectively. However, asiaticoside did not alter 4-HNE induced necrosis (Figure 15B).

The nuclear morphological analysis of untreated control, 4-HNE treated cells and 4-HNE with asiaticoside co-treated cells were shown in Figure 15A.

(A.)

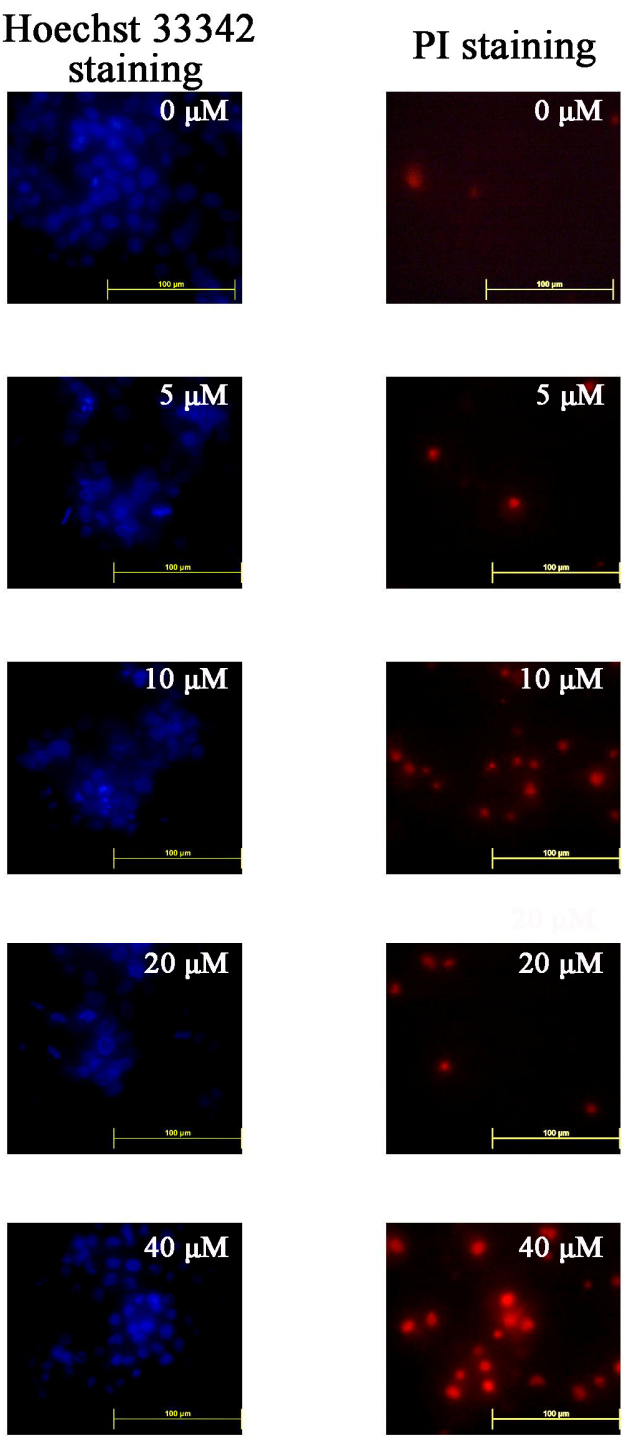
Hoechst 33342 staining
PI staining
0 μM
0 μM
5 μM
5 μM
10 μM
10 μM
20 μM
20 μM
40 μM
40 μM

(B.)

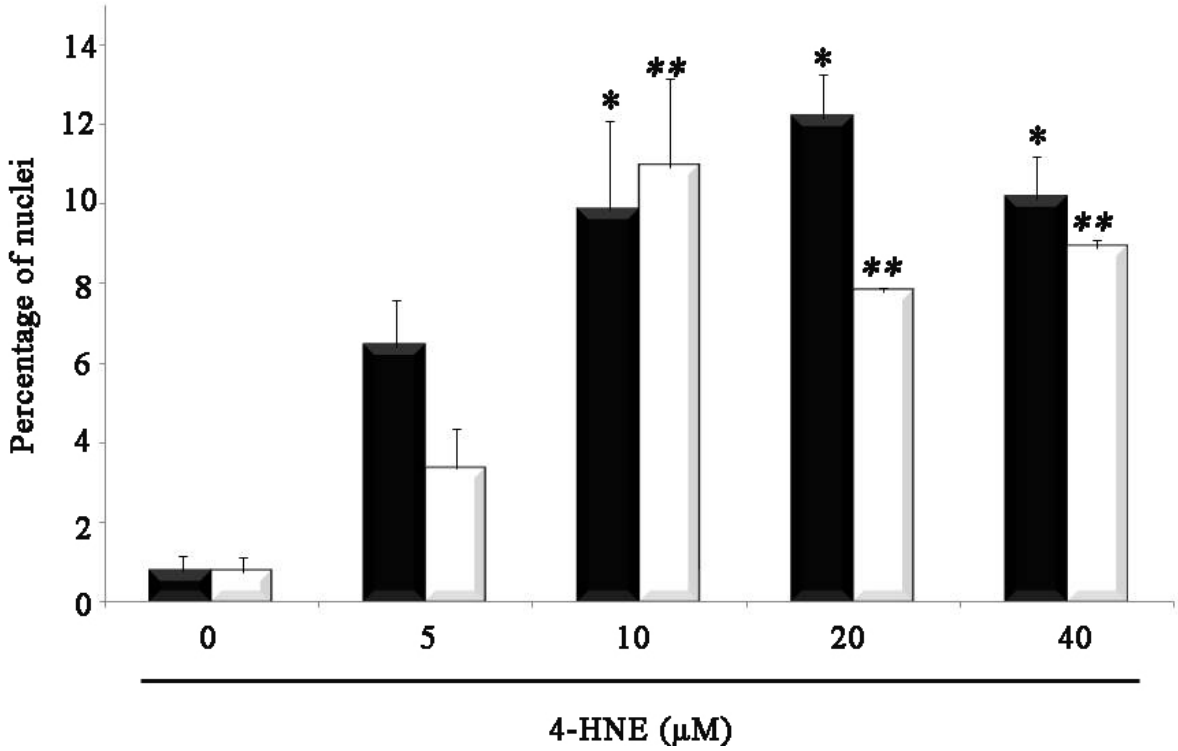

Figure 12 4-HNE induced ECV-304 apoptosis and necrosis. (A.) Cells were incubated with various concentrations of 4-HNE (0-40 μM) for 12 hours. Morphology of cell was analyzed by staining with Hoechst 33342 and PI and fluorescence images were recorded using fluorescence microscope. (B.) Cell morphology detected by Hoechst 33342 and PI staining assay. The results were expressed as mean ± S.E.M. of percentage of apoptosis (solid columns), percentage of necrosis (empty columns) determined from three independent experiments. Statistical significance: * $P < 0.05$ versus untreated control (apoptosis), ** $P < 0.05$ versus untreated control (necrosis) analyzed by repeated ANOVA and Tukey's post test.

(A.)

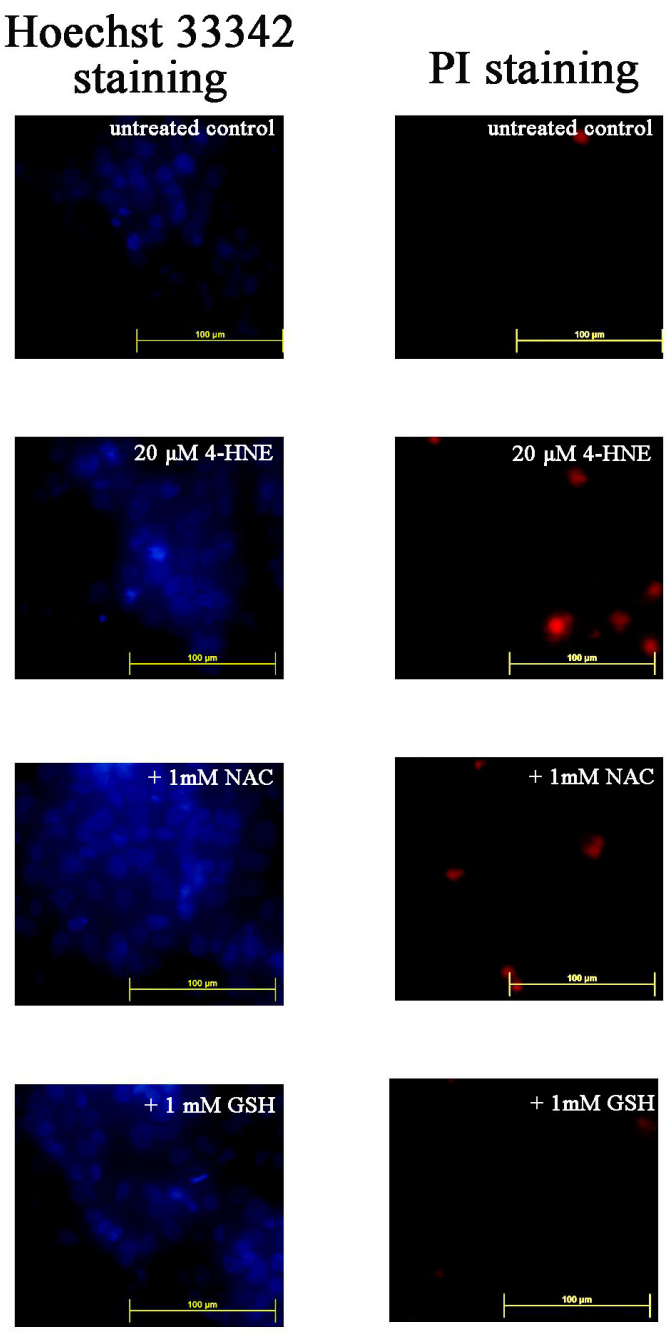
Hoechst 33342 staining
PI staining
untreated control
untreated control
20 µM 4-HNE
20 µM 4-HNE
+ 1mM NAC
+ 1mM NAC
+ 1 mM GSH
+ 1mM GSH
100 µm

(B.)

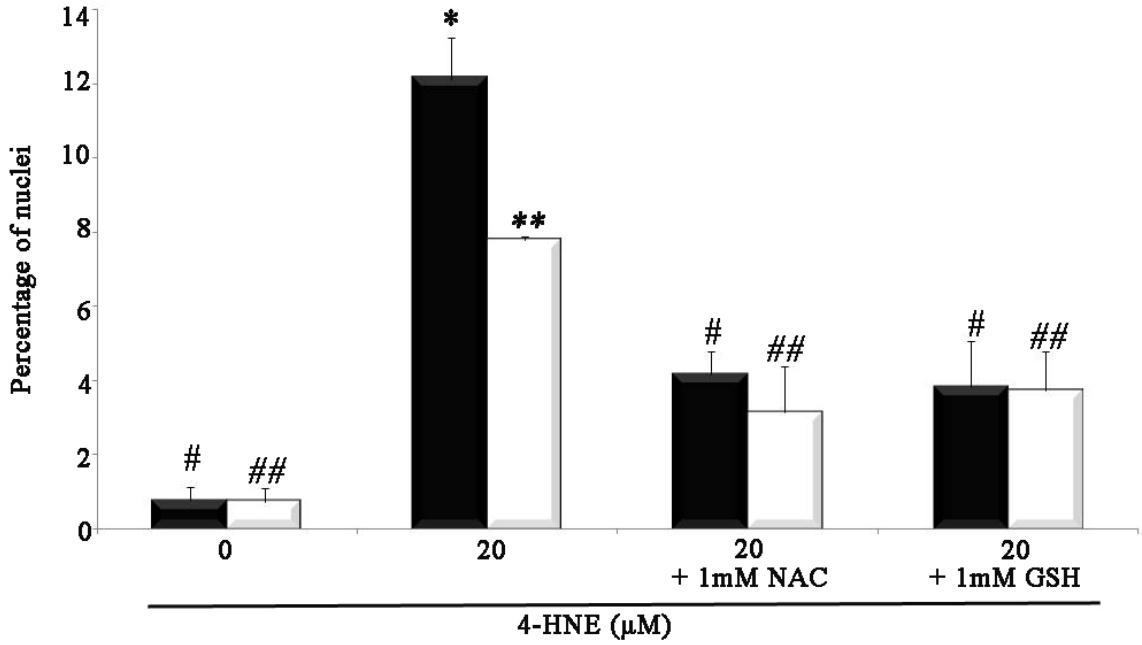

Figure 13 Effect of antioxidants on 4-HNE induced apoptosis and necrosis. (A.) The cells were co-treated with antioxidant, NAC (1mM) or GSH (1mM), and 4-HNE (20 μM) for 12 hours. Morphology of cell was analyzed by staining with Hoechst 33342 and PI and fluorescence images were recorded using fluorescence microscope. (B.) Cell morphology detected by Hoechst 33342 and PI staining assay. The results were expressed as mean ± S.E.M. of percentage of apoptosis (solid columns), percentage of necrosis (empty columns) determined from three independent experiments. Statistical significance: * $P < 0.05$ versus untreated control (apoptosis), # $P < 0.05$ versus 4-HNE (20 μM) treated group (apoptosis), ** $P < 0.05$ versus untreated control (necrosis), ## $P < 0.05$ versus 4-HNE (20 μM) treated group (necrosis) analyzed by repeated ANOVA and Tukey's post test.

(A.)

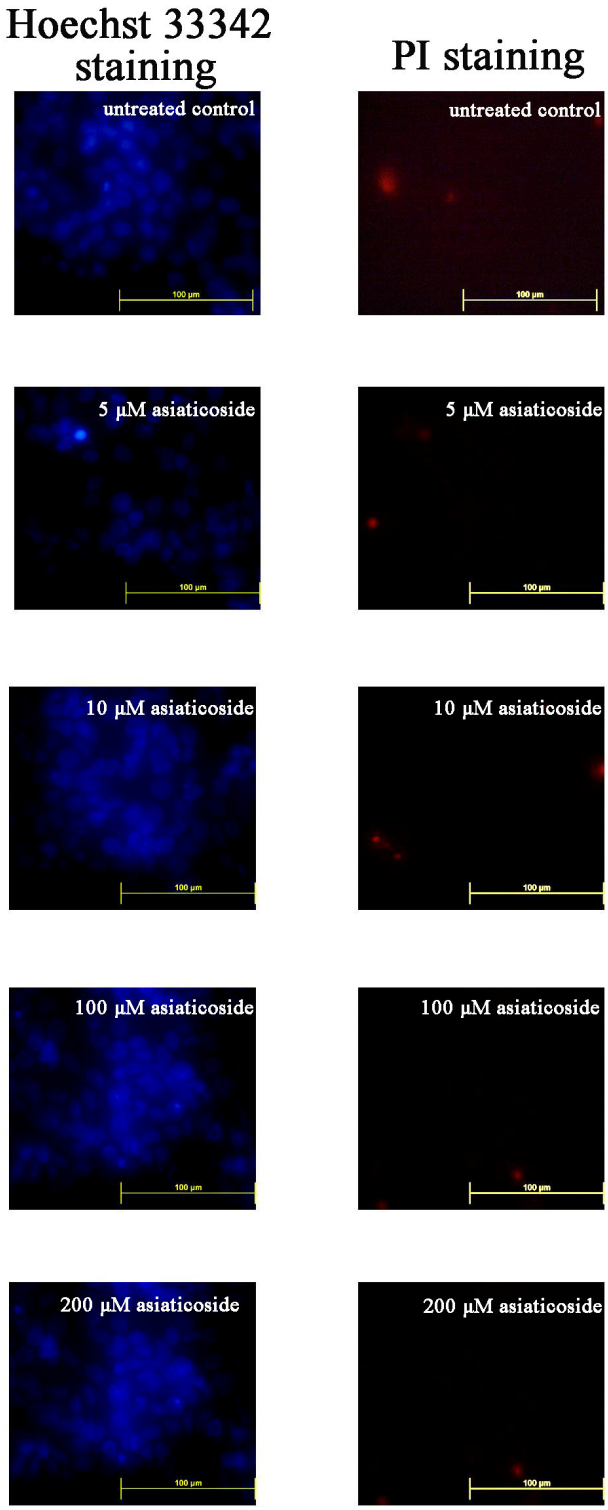
Hoechst 33342 staining
PI staining
untreated control
untreated control
5 µM asiaticoside
5 µM asiaticoside
10 µM asiaticoside
10 µM asiaticoside
100 µM asiaticoside
100 µM asiaticoside
200 µM asiaticoside
200 µM asiaticoside
100 µm

(B.)

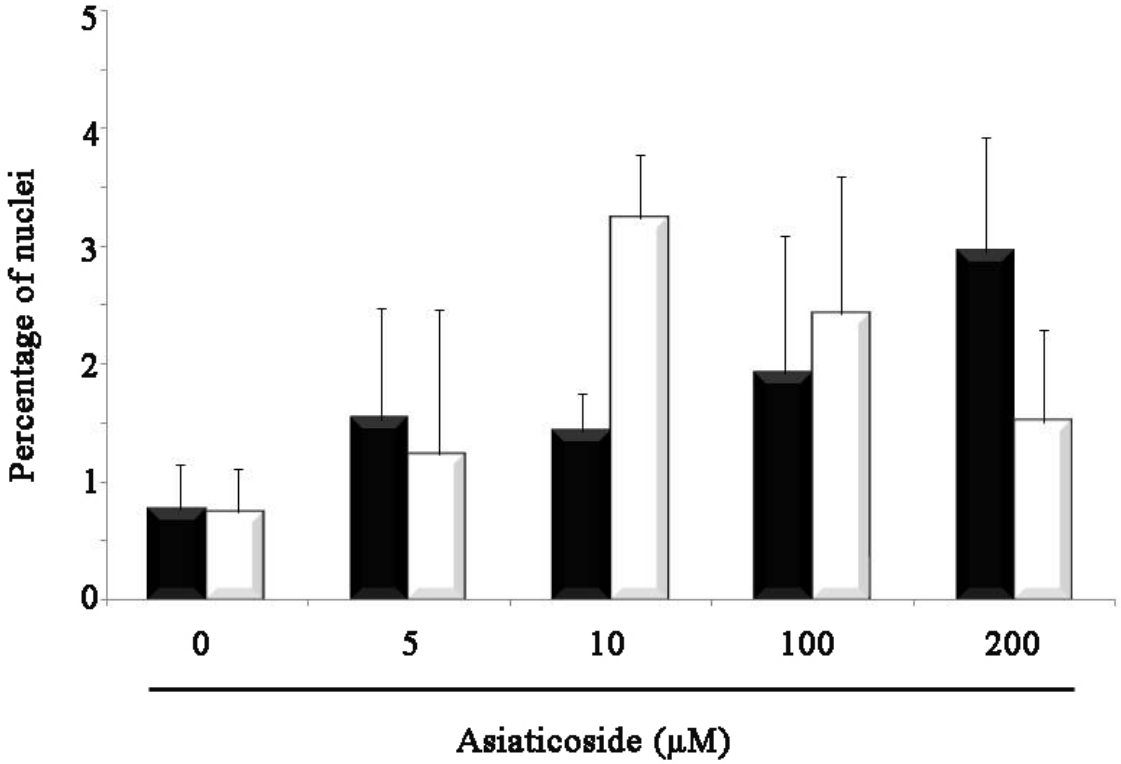

Figure 14 Effect of asiaticoside on induction of apoptosis and necrosis. (A.) The cells were incubated with various concentrations of asiaticoside (0-200 μM) for 12 hours. Morphology of cell was analyzed by staining with Hoechst 33342 and PI and fluorescence images were recorded using fluorescence microscope. (B.) Cell morphology detected by Hoechst 33342 and PI staining assay. The results were expressed as mean ± S.E.M. of percentage of apoptosis (solid columns), percentage of necrosis (empty columns) determined from three independent experiments.

(A.)

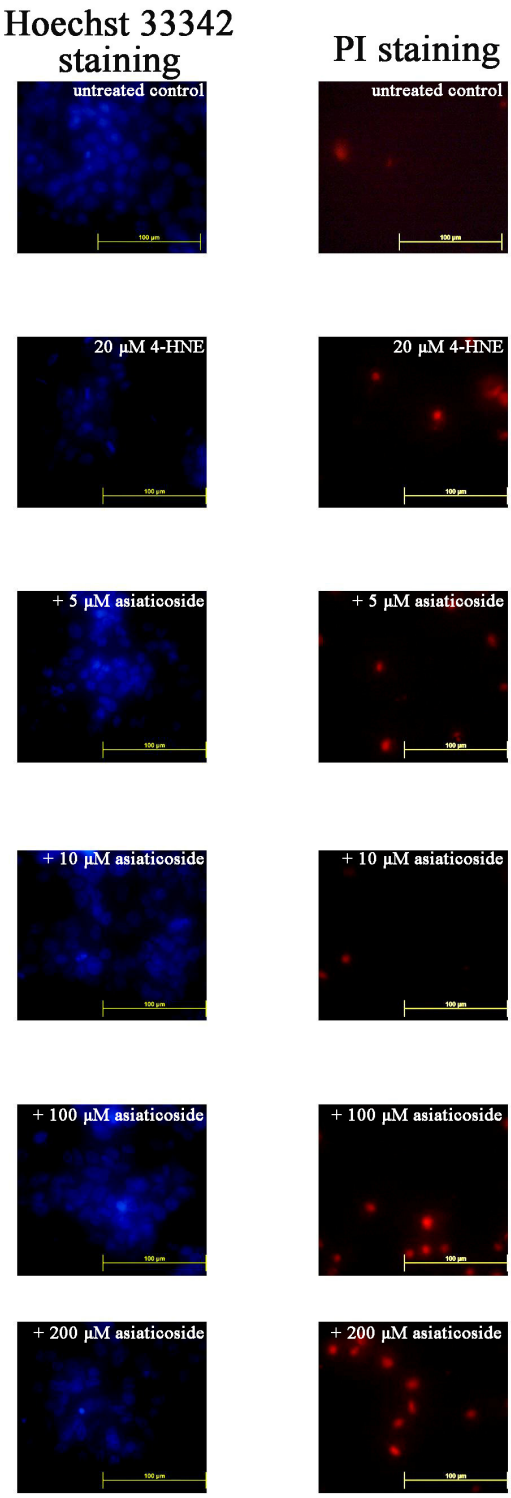
Hoechst 33342 staining
PI staining
untreated control
untreated control
20 µM 4-HNE
20 µM 4-HNE
+ 5 µM asiaticoside
+ 5 µM asiaticoside
+ 10 µM asiaticoside
+ 10 µM asiaticoside
+ 100 µM asiaticoside
+ 100 µM asiaticoside
+ 200 µM asiaticoside
+ 200 µM asiaticoside

(B.)

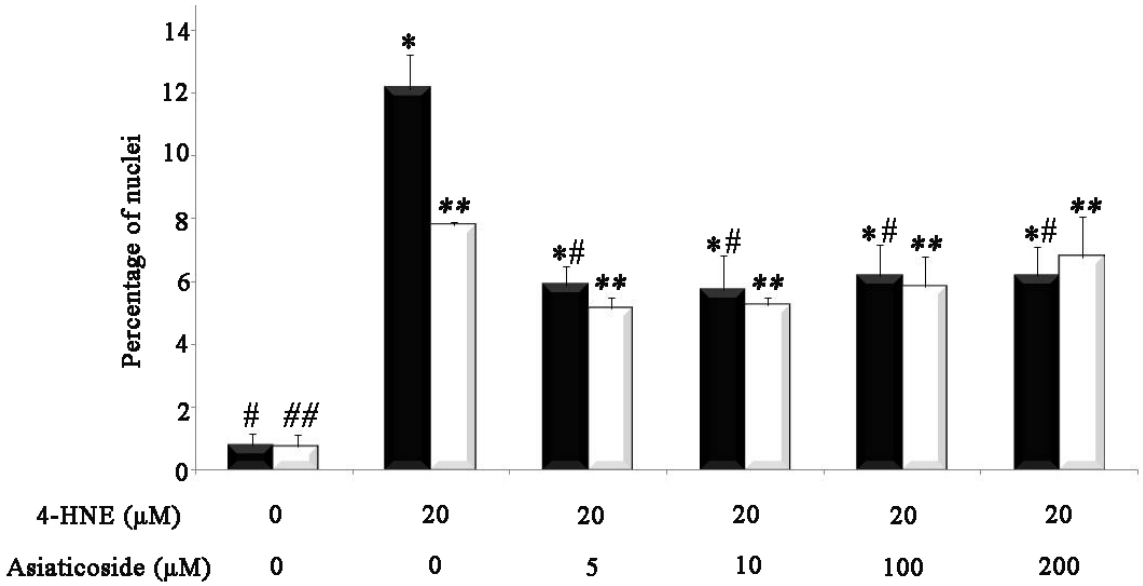

Figure 15 Effect of asiaticoside on 4-HNE induced apoptosis and necrosis. (A.) The cells were co-treated with asiaticoside (5-200 μM) and 4-HNE (20 μM) for 12 hours. Morphology of cell was analyzed by staining with Hoechst 33342 and PI and fluorescence images were recorded using fluorescence microscope. (B.) Cell morphology detected by Hoechst 33342 and PI staining assay. The results were expressed as mean ± S.E.M. of percentage of apoptosis (solid columns), percentage of necrosis (empty columns) determined from three independent experiments. Statistical significance: * $P < 0.05$ versus untreated control (apoptosis), # $P < 0.05$ versus 4-HNE (20 μM) treated group (apoptosis), ** $P < 0.05$ versus untreated control (necrosis), ## $P < 0.05$ versus 4-HNE (20 μM) treated group (necrosis) analyzed by repeated ANOVA and Tukey's post test.

3. Assay of intracellular ROS

The intracellular ROS level was determined by ROS-specific $DCFH_2$-DA fluorescence dye and analyzed with flow cytometry. In addition, the intracellular DCF fluorescence was visualized by fluorescence microscopy.

3.1 Measurement of intracellular ROS generation induced by 4-HNE

3.1.1 Time dependent study

To examine the time-course profile of 4-HNE induced ROS generation, ECV-304 cells were incubated with toxic concentration of 4-HNE (20 μM) for various incubation times (0-120 min). At each time point, intracellular ROS was measured by using flow cytometry and $DCFH_2$-DA. As shown in Figure 16A and 16B, there was gradually increased in relative DCF fluorescence from 30 minutes (1.36 ± 0.05) to 120 minutes (1.77 ± 0.09).

The time course profile of 4-HNE induced intracellular ROS was further examined by visual analysis using fluorescence microscope. As shown in Figure 16C, the DCF intensity of 4-HNE treated cells gradually increased and reached its maximum level at 120 min.

3.1.2 Concentration dependent study

ECV-304 cells were treated with various concentrations of 4-HNE (0-40 μM) and intracellular ROS was measured after 120 minutes by using flow cytometry and $DCFH_2$-DA. The concentrations of 4-HNE at 10, 20 amd 40 μM significantly increased ($P < 0.05$) intracellular ROS generation as determined by the increase in the relative DCF intensity to 1.26 ± 0.05, 1.38 ± 0.07, 1.46 ± 0.03, respectively, as compared to untreated control. (Figure 17A, 17B)

To further examine the 4-HNE induced intracellular ROS production, the intracellular ROS formation was visualized by using fluorescence microscopy. As indicated in Figure 17C, 4-HNE enhanced intracellular DFC fluorescence as compared to untreated control.

3.2 Effect of antioxidants on 4-HNE induced intracellular ROS generation

To examine whether the antioxidants effectively inhibited 4-HNE induced intracellular ROS formation, the intracellular ROS formation in response to the antioxidants was determined at 120 minutes by using $DCFH_2$-DA fluorescence dye and flow cytometry. As illustrated in Figure 18A and 18B, the cells incubated with 4-HNE (20 μM) dramatically increased DCF intensity to 1.38 ± 0.07. Addition of antioxidant, NAC (1 mM) or GSH (1 mM), almost reduced DCF intensity to the control level. The antioxidant NAC completely inhibited 4-HNE induced ROS formation with decreased DCF intensity to 0.91 ± 0.08 as well as GSH decreased DCF intensity to 0.90 ± 0.12.

The effect of antioxidants on 4-HNE induced intracellular ROS formation was further investigated by visual analysis using fluorescence microscope. As shown in Figure 18C, exposure of cells to NAC or GSH with 4-HNE revealed a decrease in the intensity of DCF fluorescence.

3.3 Effect of asiaticoside on 4-HNE induced intracellular ROS generation

To determine whether asiaticoside could inhibit intracellular ROS generation induced by 4-HNE, ECV-304 cells were treated with toxic concentration of 4-HNE (20 μM) in the presence or absence of asiaticoside (0-200 μM) and the intracellular ROS formation was determined at 120 minutes by $DCFH_2$-DA fluorescence dye and flow cytometry. Addition of 200 μM asiaticoside reduced the DCF intensity to 2.30 ± 0.14 as compared to 4-HNE treated cells (3.43 ± 0.21) (Figure 19A, 19B).

The effect of asiaticoside on 4-HNE induced intracellular ROS formation was further examined by visual analysis using fluorescence microscope. As illustrated in

Figure 19C, exposure of cells to asiaticoside with 4-HNE revealed a reduction in the intensity of DCF fluorescence.

(A)

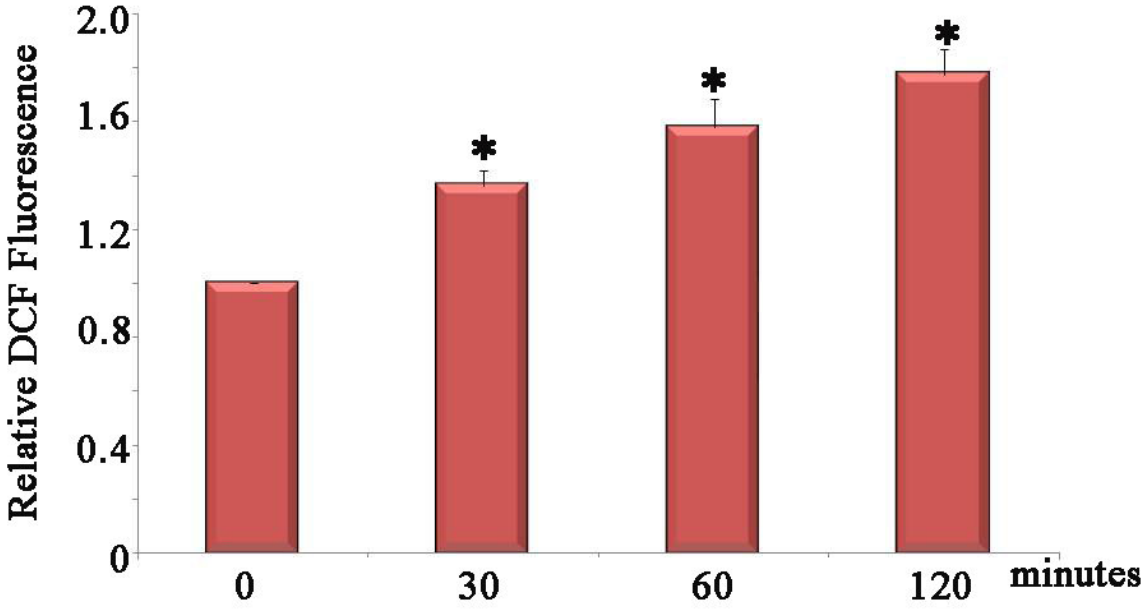
Relative DCF Fluorescence
2.0
1.6
1.2
0.8
0.4
0
*
*
*
0
30
60
120
minutes

(B)

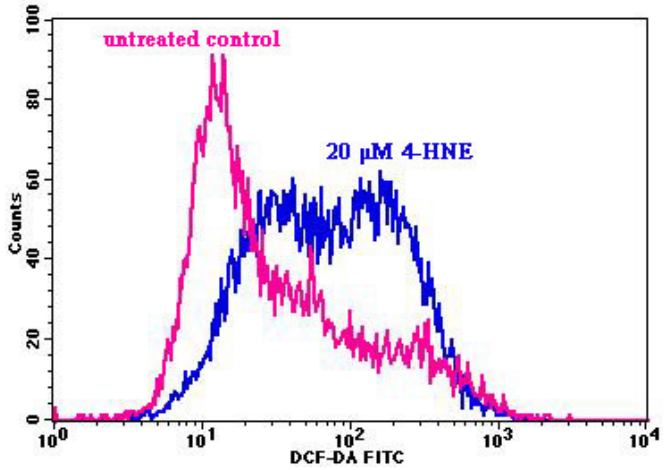
untreated control
20 µM 4-HNE
Counts
100
80
60
40
20
0
10^0
10^1
10^2
10^3
10^4
DCF-DA FITC

(C)

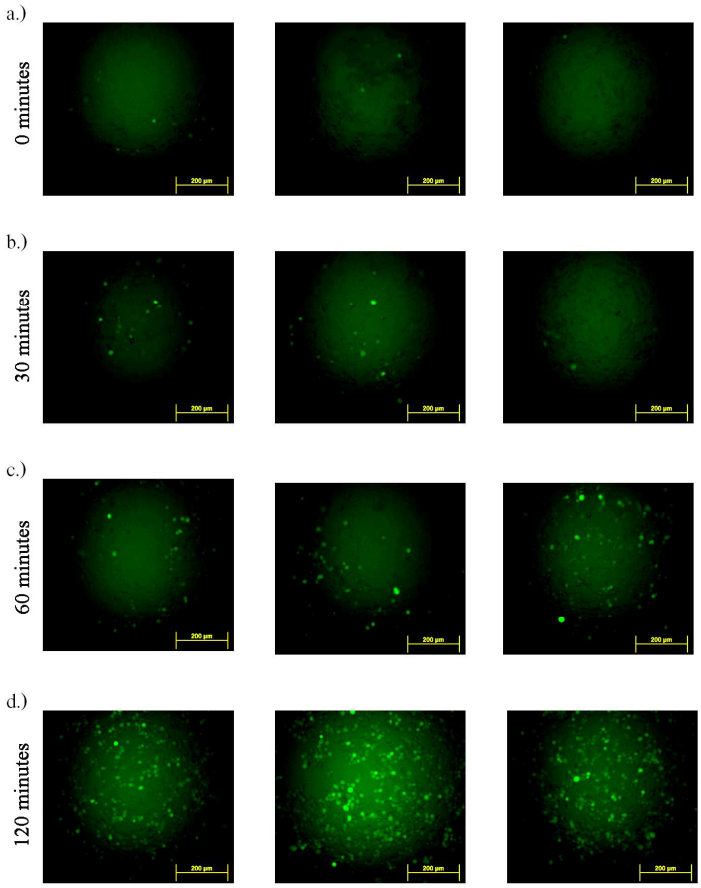

Figure 16 Time-course profile of ROS formation in 4-HNE treated cells. (A) The cells were incubated with 4-HNE (20 μM) at various incubation times (0-120 minutes). The intracellular ROS level was determined by using $DCFH_2$-DA fluorescence dye stain and analyzed by flow cytometry. The results were expressed as mean ± S.E.M of relative DCF fluorescence determined from three independent experiments. Statistical significance: * $P < 0.05$ versus untreated control analyzed by repeated ANOVA and Tukey's post test. (B) The graphs are representatives of 4-HNE mediated ROS formation at 120 minutes. (C) Fluorescence micrographs of intracellular ROS generation in ECV-304 cells treated with 4-HNE (20 μM) at various incubation times (0-120 minutes).

(A)

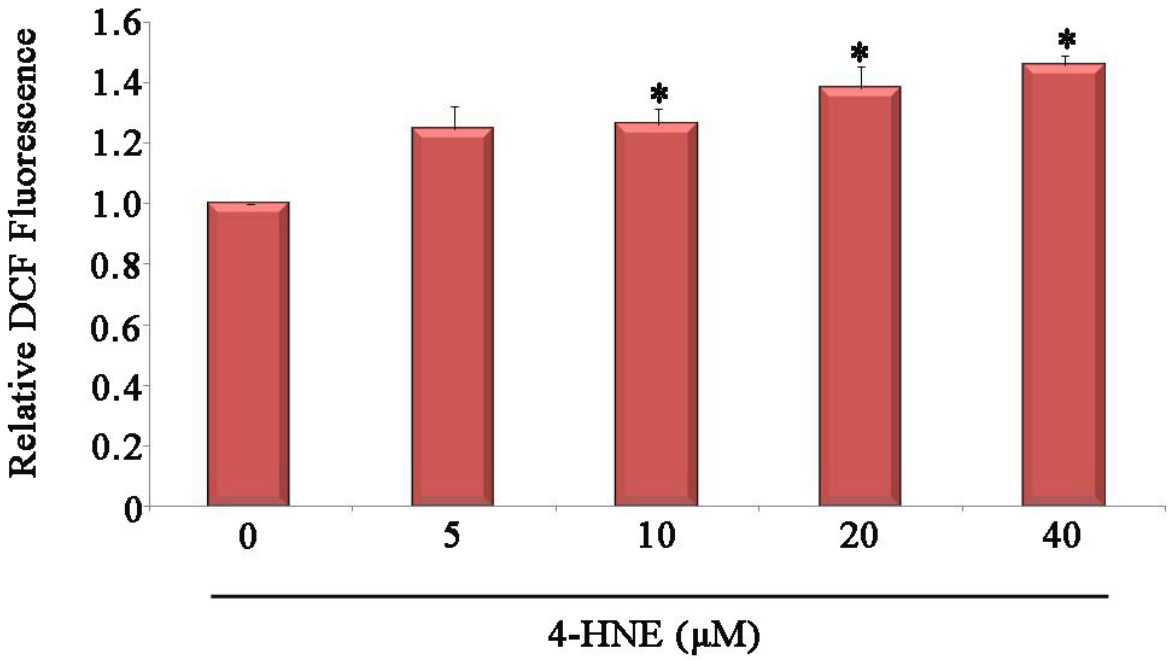
Relative DCF Fluorescence
1.6
1.4
1.2
1.0
0.8
0.6
0.4
0.2
0
*
*
*
0
5
10
20
40
4-HNE (μM)

(B)

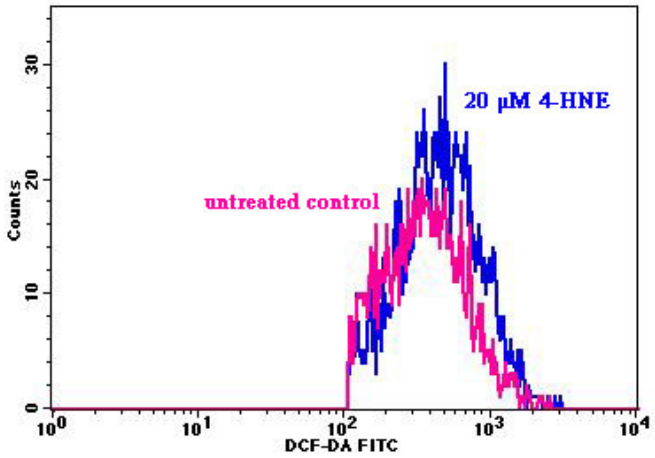
20 μM 4-HNE
untreated control
Counts
30
20
10
0
10^0
10^1
10^2
10^3
10^4
DCF-DA FITC

(C)

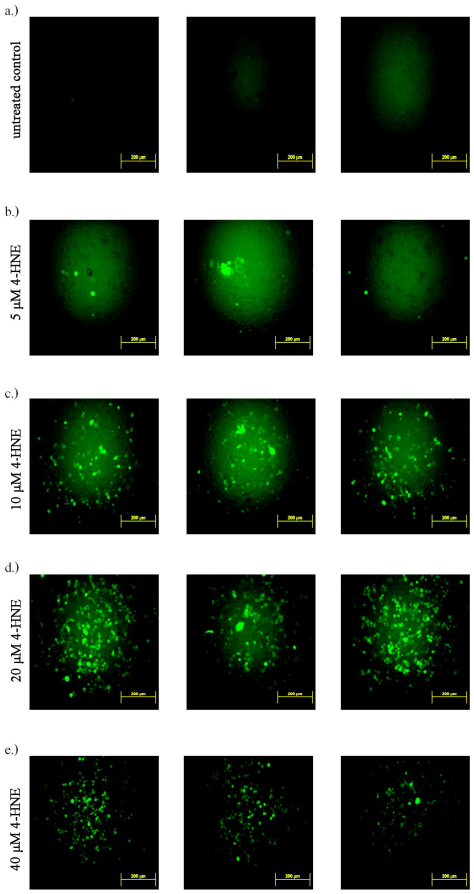

Figure 17 Effect of 4-HNE on ROS formation in ECV-304 cells. (A) The cells were incubated with various concentrations of 4-HNE (0-40 µM) for 120 minutes. The intracellular ROS level was determined by using $DCFH_2$-DA fluorescence dye stain and analyzed by flow cytometry. The results were expressed as mean ± S.E.M of relative DCF fluorescence determined from three independent experiments. Statistical significance: * $P < 0.05$ versus untreated control analyzed by repeated ANOVA and Tukey's post test. (B) The graphs are representatives of 4-HNE induced ROS generation. Cells were incubated with 4-HNE (20 µM) for 120 minutes. (C) Fluorescence micrographs of intracellular ROS generation in ECV-304 cells treated with various concentrations of 4-HNE (0-40 µM) for 120 minutes.

(A)

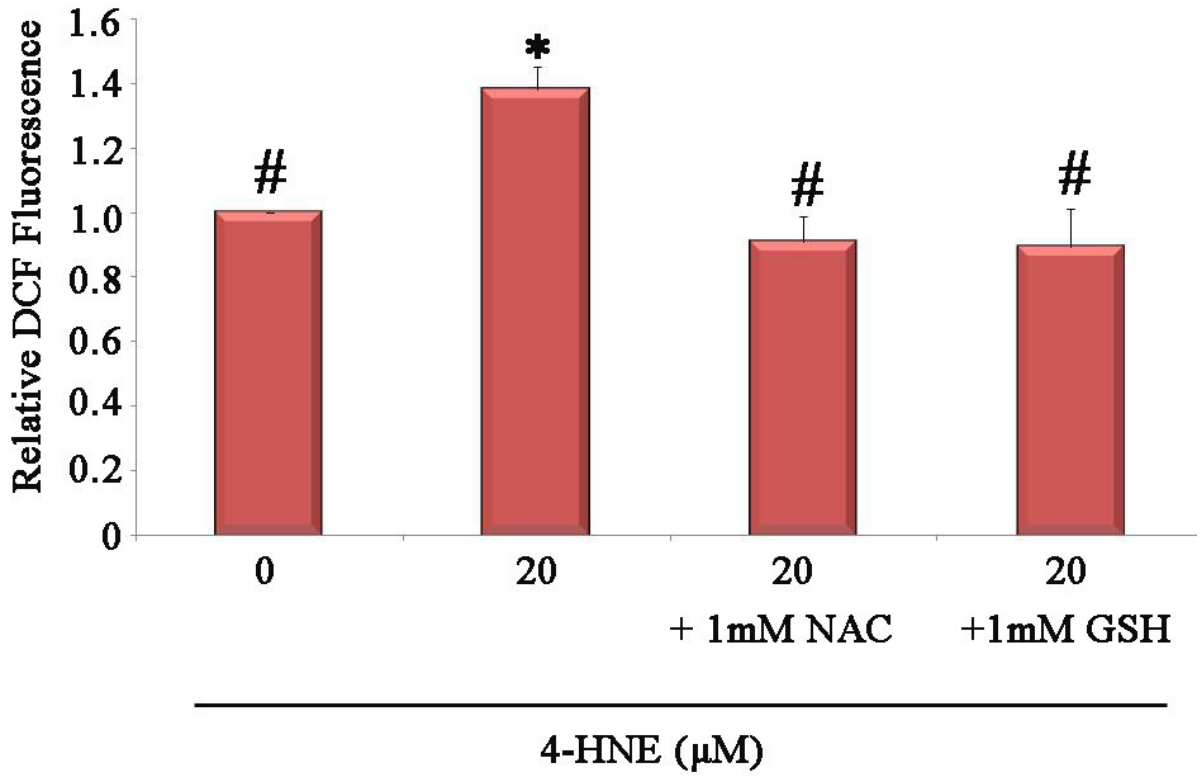
Relative DCF Fluorescence
1.6
1.4
1.2
1.0
0.8
0.6
0.4
0.2
0
#
*
#
#
0
20
20
+ 1mM NAC
20
+1mM GSH
4-HNE (μM)

(B)

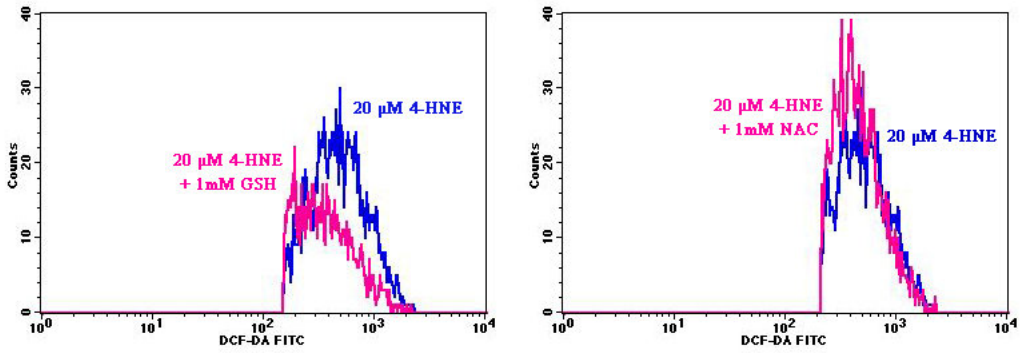
20 μM 4-HNE
20 μM 4-HNE
+ 1mM GSH
Counts
DCF-DA FITC
20 μM 4-HNE
+ 1mM NAC
20 μM 4-HNE
Counts
DCF-DA FITC

(C)

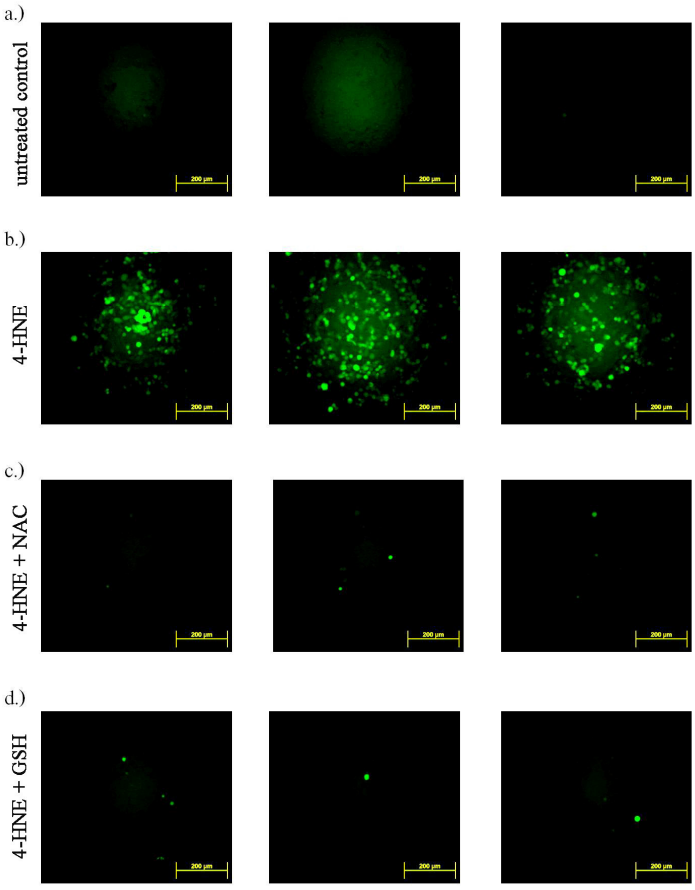

Figure 18 Effect of antioxidants on 4-HNE induced ROS formation in ECV-304 cells. (A) The cells were co-treated with antioxidants, NAC (1mM) or GSH (1 mM), and 4-HNE (20 μM) for 120 minutes. The intracellular ROS level was determined by using $DCFH_2$-DA fluorescence dye stain and analyzed by flow cytometry. The results were expressed as mean ± S.E.M of relative DCF fluorescence determined from three independent experiments. Statistical significance: * $P < 0.05$ versus untreated control, # $P < 0.05$ versus 4-HNE (20 μM) treated group analyzed by repeated ANOVA and Tukey's post test. (B) The graphs are representatives of the inhibition effects of antioxidant on 4-HNE induced ROS generation. Cells were co-treated with antioxidant, NAC (1mM) or GSH (1 mM), and 4-HNE (20 μM) for 120 minutes. (C) Fluorescence micrographs of intracellular ROS generation induced by 4-HNE (20 μM) in ECV-304 cells in the presence or absence of antioxidants (NAC, 1 mM or GSH, 1 mM) and 4-HNE for 120 minutes.

(A)

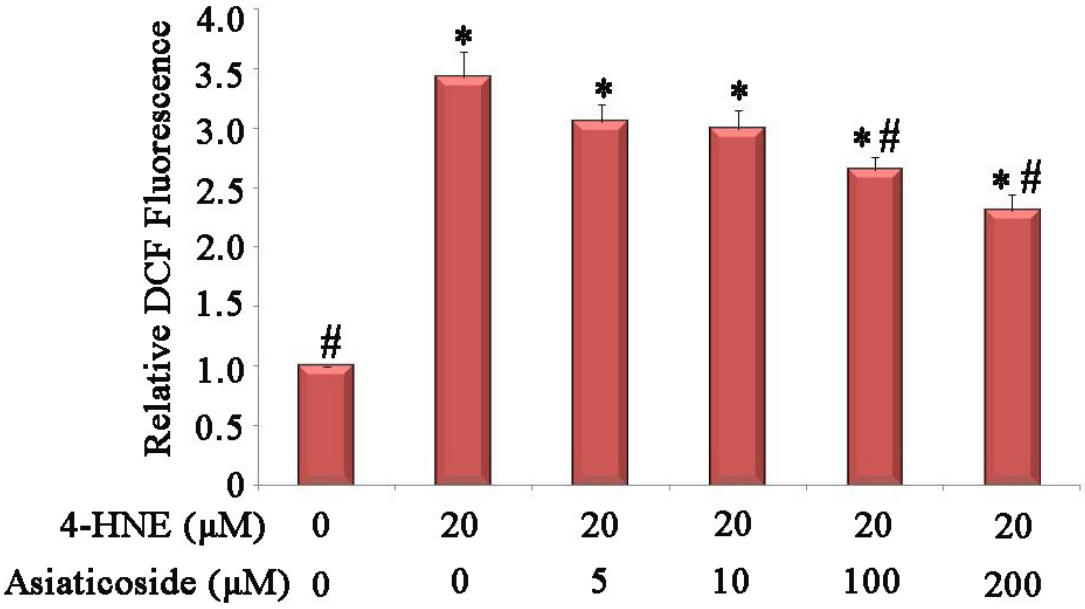
Relative DCF Fluorescence
4.0
3.5
3.0
2.5
2.0
1.5
1.0
0.5
0
*
*
*
*#
*#
#
4-HNE (μM) 0 20 20 20 20 20
Asiaticoside (μM) 0 0 5 10 100 200

(B)

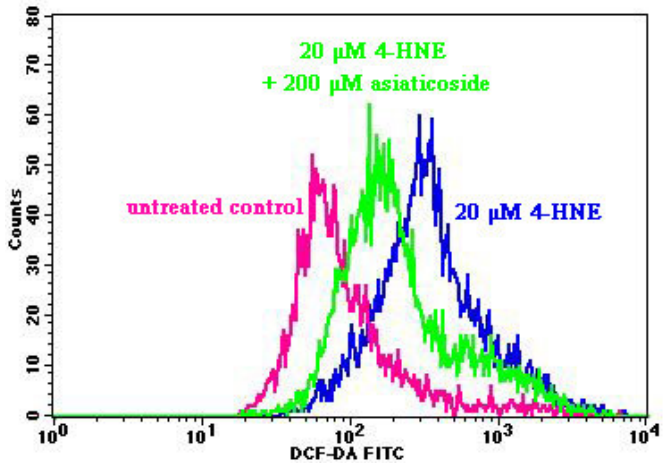
20 μM 4-HNE
+ 200 μM asiaticoside
untreated control
20 μM 4-HNE
Counts
DCF-DA FITC

(C)

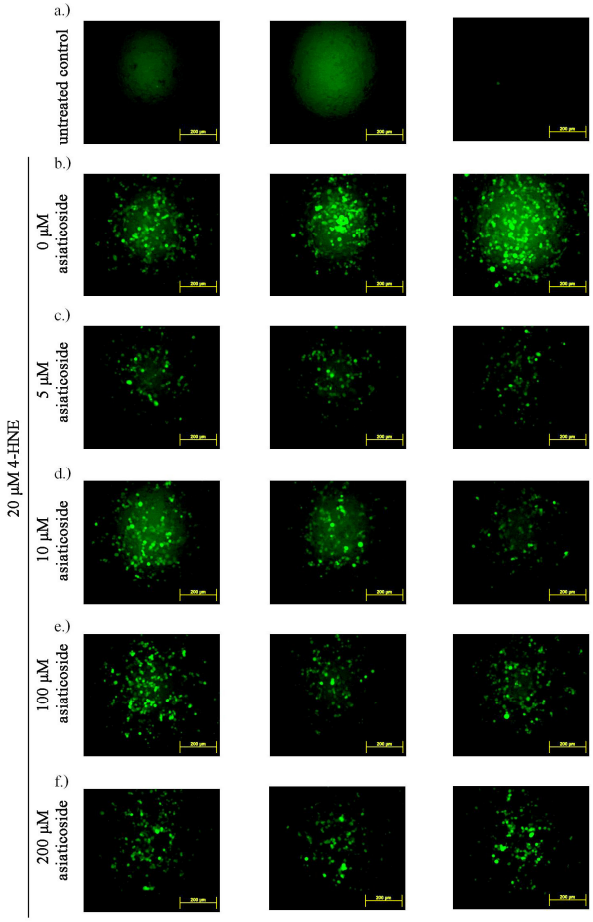

Figure 19 Effect of asiaticoside on 4-HNE induced ROS formation in ECV-304 cells. (A) The cells were co-treated with various concentrations of asiaticoside (0-200 µM), and 4-HNE (20 µM) for 120 minutes. The intracellular ROS level was determined by using $DCFH_2$-DA fluorescence dye stain and analyzed by flow cytometry. The results were expressed as mean ± S.E.M of relative DCF fluorescence determined from three independent experiments. Statistical significance: * $P < 0.05$ versus untreated control, # $P < 0.05$ versus 4-HNE (20 µM) treated group analyzed by repeated ANOVA and Tukey's post test. (B) The graphs are representatives of the inhibition effects of asiaticoside on 4-HNE induced ROS generation. Cells were co-treated with asiaticoside (200 µM) and 4-HNE (20 µM) for 120 minutes. (C) Fluorescence micrographs of intracellular ROS generation in ECV-304 cells co-treated with various concentrations of asiaticoside (0-200 µM), and 4-HNE (20 µM) for 120 minutes.

CHAPTER V
DISCUSSION AND CONCLUSION

A major finding of this study was that 4-HNE exerted a toxic effect on ECV-304 cells in a concentration dependent manner, as determined by MTT assay, Hoechst 33342 and PI staining assay. Exposure of ECV-304 cells to 4-HNE resulted in a dramatic increase in intracellular ROS level, which led to cell apoptosis and necrosis. Moreover, the involvement of ROS generated by 4-HNE and its cytotoxic effect were established by which addition of antioxidants, NAC or GSH, dramatically blocked 4-HNE induced ROS up-regulation as well as cell death.

Several studies have indicated the role of 4-HNE, a major product of lipid peroxidation, as a strong oxidant **(24-28)**. Moreover, a number of studies reported that 4-HNE plays an important role in many pathological conditions, such as cancer **(7)**, neurodegenerative diseases **(14, 23)** and vascular diseases **(3, 4, 57)**. Indeed, 4-HNE has been found after lipid peroxidation of the cell membrane. Together with these findings, the possible underlying mechanisms of 4-HNE in regulation of pathological processes may cause by its ability to propagate and increase oxidative stress in surrounding tissues and cells. ROS have been shown to be implicated in several vascular disorders, including hypertension **(69)**, diabetes **(70)**, atherosclerosis **(71, 72)**. Since, the molecular mechanism and its exact role of 4-HNE on vascular cell damage have not yet been clearly elucidated, the aim of this study is to identify the regulatory mechanism of 4-HNE and its implication in ECV-304 endothelial cells.

To investigate the cytotoxicity of 4-HNE on ECV-304 cells, MTT assay was performed. MTT assay is colorimetric assay and is widely used for study of cell viability and cell proliferation as well as cytotoxicity. This assay measures the metabolic activity of mitochondrial dehydrogenase enzymes in viable cells. The present study showed that 4-HNE caused a significant decrease in cell viability in concentration dependent manner (Figure 8).

To confirm cytotoxic effect of 4-HNE and to provide more information about cell damage, cell death detections were further performed. Apoptosis and necrosis were

identified as two major mechanisms of cell death and were linked to several pathological processes **(73-76)**. These events have distinct mechanisms with very different cellular and biologic characteristics. Apoptosis is a normal occurrence in which an orchestrated sequence of events leads to the death of a cell. Apoptosis is defined by characteristic changes in the nuclear morphology, including chromatin condensation (pyknosis) and fragmentation (karyorrhexis); minor changes in cytoplasmic organelles; and overall cell shrinkage, blebbing of the plasma membrane and formation of apoptotic bodies that contain nuclear or cytoplasmic material **(77)**. In contrast to apoptosis, cells that die in response to severe and acute injuries or extreme physicochemical injuries exhibit very different morphological changes, referred as necrosis. Typically, the morphological changes of the cells that undergo this process include cell swelling; formation of cytoplasmic vacuoles; distended endoplasmic reticulum; formation of cytoplasmic blebs; condensed, swollen or ruptured mitochondria; disaggregation and detachment of ribosomes; disrupted organelle membranes; swollen and ruptured lysosomes; and eventually disruption of the cell membrane **(59)**. Based on these distinctions, various methods have been developed to identify cells undergoing apoptosis and necrosis. Among these, the usefulness of the Hoechst 33342 and propidium iodide staining assay for studying apoptosis and necrosis, respectively, have been demonstrated in a number of previous studies. Hoechst 33342, a cell permeable DNA dye, is a widely accepted method to detect DNA condensation as well as fragmentation, important features of apoptotic cells **(78)**. Propidium iodide (PI), a cell impermeable dye, was used to identify necrotic cells due to PI's property which penetrate only membrane-damaged cells, an important characterization of necrotic cells **(79)**. The present study showed that 4-HNE was able to induce both apoptosis as well as necrosis in ECV-304 cells (Figure 12).

Recently, the possible mechanism of 4-HNE induced cell death has been proposed by Lee, J.Y., et al. **(28)**. They showed that vascular smooth muscle cell generated high level of intracellular ROS from mitochondria after treatment with 4-HNE and these intracellular ROS were responsible for cell death. Consistent with the previous report, the present study found the involvement of ROS in 4-HNE mediated cell damge in endothelial ECV-304 cells. Nevertheless, only apoptotic cell death was detected in response to low concentration of 4-HNE (10 μM) in vascular smooth muscle cell reported

by Lee, J.Y., et al.**(28)**, whereas, 10 μM of 4-HNE induced both apoptosis and necrosis in ECV-304 cells in this study. Many studies indicated the widely accepted concept that a low intracellular ROS level generally leads to cell apoptosis and a high intracellular ROS level caused cell necrosis. Thus, it was suggested that antioxidant machinery in these two cells (vascular smooth muscle cell and endothelial cell) may differ. Many cellular enzymes have been shown to implicate in ROS reducing mechanisms, for example, catalase, superoxide dismutase, glutathione peroxidases **(2)**. The expression levels of these antioxidant enzymes are likely to determine the susceptibility of cells to ROS induced cell damage. Hence, the necrotic cell death at low concentration of 4-HNE (10 μM) in ECV-304 cells may reflect the lower antioxidant system, as compared to the vascular smooth muscle cells.

4-HNE induced intracellular ROS generation has been reported by many research groups **(24-28)**; however, its oxidant effect in vascular ECV-304 cells is still largely unknown. The present study demonstrated that there was an increase of intracellular ROS level, in response to 4-HNE in both concentration and time dependent manner, evaluated as an increased intensity of DCF fluorescence (Figure 16, 17).

The present study also determined the correlation between 4-HNE cytotoxicity and its oxidant effect. Co-treatment with pan antioxidant (NAC or GSH) and 4-HNE resulted in an increase in cell viability, analyzing by MTT assay (Figure 10). Moreover, addition of antioxidant decreased intracellular ROS induced by 4-HNE (Figure 18), and subsequently reduced cell death (Figure 13), suggesting a strong correlation between ROS up-regulation and 4-HNE cytotoxicity.

Centella asiatica (Buabok) is claimed to posses several pharmacological activities, such as, anti-inflammatory **(29)**, memory improvement **(30, 31)**, and anticancer activity**(32)**. Its major active components are triterpene saponins, asiaticoside and medecassoside, and their aglycones, asiatic acid and medecassic acid **(39)**. Asiaticoside, the most abundant triterpene glycoside in *C. asiatica*, was shown to have several potential pharmacological properties, including anxiolytic **(42)**, wound healing **(40)**, and antioxidant **(41)**. In the present study, asiaticoside significantly protected ECV-304 cells from 4-HNE induced cell damage (Figure 11). However, the Hoechst 33342 and PI staining assays indicated that only apoptotic cell death could be reduced by the addition

of asiaticoside (Figure 15). Moreover, these results showed that protective effect of asiaticoside was not related to its antioxidant property, since asiaticoside at the concentration of 100 μM showed a higher protective effect than the concentration at 10 μM, while, there was no significant difference in antioxidant effect between concentration at 10 μM and 100 μM of asiaticoside. Besides, there were no significant alterations in apoptotic and necrotic cell detection in response to the co-treatment of 4-HNE and various concentration of asiaticoside (5-200 μM). These results suggested that antioxidant effect of asiaticoside may not play a critical role on its protective mechanisms against 4-HNE induced ECV-304 cell damage.

In conclusion, the present study provided the evidence that the intracellular ROS generated by 4-HNE was strongly responsible to its cytotoxic effects. Moreover, asiaticoside, a major component of *Centella asiatica*, showed a strong protective effect against 4-HNE induced ECV-304 cell death. However, the precise mechanism by which asiaticoside in protection of 4-HNE induced cytotoxicity remains to be defined.

REFERENCES

(1) Uchida, K. 4-Hydroxy-2-nonenal: a product and mediator of oxidative stress. Progress in Lipid Research 42(4) (2003): 318-43.

(2) Yang, Y., Sharma, R., Sharma, A., Awasthi, S., and Awasthi, Y.C. Lipid peroxidation and cell cycle signaling: 4-hydroxynonenal, a key molecule in stress mediated signaling. Acta Biochimica Polonica 50(2) (2003): 319-36.

(3) Itakura, K., et al. Detecttion of lipofuscin-like fluorophore in oxidized human low-density lipoprotein. FEBS Letters 473 (2000): 249-253.

(4) Palinski, W., et al. Antisera and monoclonal antibodies specific for epitopes generated during oxidative modification of density lipoprotein. Arteriosclerosis Thrombosis, and Vascular Biology 10 (1990): 325-335.

(5) Yang, Y., et al. Glutathione-S-transferase A4-4 modulates oxidative stress in endothelium: possible role in human atherosclerosis. Atherosclerrosis 173 (2004): 211-221.

(6) McConnell, E.J. and Raess, B.U. Intracellular Ca^{2+} Homeostatic Regulation and 4-Hydroxynonenal-Induced Aortic Endothelial Dysfunction. Endothelium 9 (2002): 45-53.

(7) Feng, Z., Hu, W., and Tang, M.-s. Trans-4-hydroxy-2-nonenal inhibits nucleotide excision repair in human cells: A possible mechanism for lipid peroxidation-induced carcinogenesis. PNAS 101(23) (2004): 8598-8602.

(8) Rahman, I., et al. 4-Hydroxy-2-Nonenal, a specific lipid peroxidation product, is elevated in lungs of patients with chronic obstructive pulmonary disease. American Journal of Respiratory and Critical Care Medicine 166 (2002): 490-495.

(9) Rytila, P., et al. Increase oxidative stress in asymptomatic current chronic smokers and GOLD stage o COPD. Respiratory Research 7(69) (2006).

(10) Kirkham, P. and Rahman, I. Oxidative stress in asthma and COPD: Antioxidants as therapeutic strategy. Phamacology & Therapeutics 111 (2006): 476-494.

(11) Harju, T., et al. Manganese superoxide dismutase is increased in the airway of smokers lungs. European Respiratory Journal J 24 (2004): 765-771.

(12) Kirkham, P.A., Spooner, G., Rahman, I., and Rossi, A.G. Macrophage phagocytosis of apoptotic neutrophils is compromised by matrix proteins modified by cigarette smoke and lipid peroxidation products. Biochemical and Biophysical Research Communications 318 (2004): 2004.

(13) Kaizaki, A., Tanaka, S., Ishige, K., Numazawa, S., and Yoshida, T. The neuroprotective effect of heme oxygenase (HO) on oxidative stress in HO-1 siRNA-transfected HT22 cells. Brain research 1108 (2006): 39-44.

(14) Yoritaka, A., et al. Immunohistochemical detection of 4-hydroxynonenal protein adducts in Parkinson disease. PNAS 93 (1996): 2696-2701.

(15) McGrath, L.T., et al. Increased oxidative stress in Alzheimer's disease as assessed with 4-hydroxynonenal but not malonaldehyde. Q J Med 94 (2001): 485-490.

(16) Siegel, S.J., Bieschke, J., Powers, E.T., and Kelly, J.W. The oxidative stress metabolite 4-hydroxynonenal promotes alzheimer protofibril formation. Biochemistry 46 (2007): 1503-1510.

(17) Kruman, I., Bruce-Keller, A.J., Bredesen, D., Waeg, G., and Mattson, M.P. Evidence that 4-hydroxynonenal mediates oxidative stress induced neuronal apoptosis. The Journal of Neuroscience 17(13) (1997): 5089-5100.

(18) Bharath, S., Hsu, M., Kaur, D., Rajagopalan, S., and Andersen, J.K. Glutathione, iron and Parkinson's disease. Biochemical Pharmacology 64 (2002): 1037-1048.

(19) Baldwin, S.A., et al. The presence of 4-hydroxynonenal/protein complex as an inicator of oxidative stress after experimental spinal cord contusion in rat model. Journal of Neurosergery 88 (1998): 874-883.

(20) Lovell, M.A., Ehmann, W.D., Mattson, M.P., and Markesbery, W.R. Elevated 4-Hydroxynonenal in Ventricular Fluid in Alzheimer's Disease. Neurobiology of Aging 18(5) (1997): 457-461.

(21) Bruckner, S.R., Perry, G., and Estus, S. 4-Hydroxynonenal contributes to NGF withdrawal-induced neuronal apoptosis. Journal of neurochemistry 85 (2003): 999-1005.

(22) Mattson, M.P. Pathways towards and away from Alzheimer's disease. Nature 430 (2004): 631-639.

(23) Sayre, L.M., et al. 4-Hydroxynonenal-derived advanced lipid peroxidation end products are increased in Alzheimer's disease. Journal of neurochemistry 68 (1997): 2092-2097.

(24) Kondo, M., Oya-Ito, T., Kumagai, T., Osawa, T., and Uchida, K. Cyclopentenone Prostaglandins as Potential Inducers of Intracellular Oxidative Stress. Journal of Biological Chemistry 276(15) (2001): 12076-12083.

(25) Usatyuk, P.V., et al. Redox regulation of 4-hydroxy-2-nonenal-mediated endothelial barrier dysfunction by focal adhesion, adherens, and tight junction proteins Journal of Biological Chemistry 281(46) (2006): 35554-66.

(26) Uchida, K., et al. Activation of stress signaling pathways by the end product of lipid peroxidation. Journal of Biological Chemistry 274(4) (1999): 2234-2242.

(27) Feng, Q., et al. Anticarcinogenic antioxidants as inhibitors against intracellular oxidative stress. Free Radical Research 35 (2001): 779-788.

(28) Lee, J.Y., et al. 4-Hydroxynonenal induces vascular smooth muscle cell apoptosis through mitochondrial generation of reactive oxygen species. Toxicology Letters 166(3) (2006): 212-221.

(29) Suguna, L., Sivakumar, P., and Chandrakasan, G. Effects of *Centella asiatica* extract on dermal wound healing in rats. Indian Journal of Experimental Biology 34(12) (1996): 1208-11.

(30) Gupta, Y.K., Kumar, M.H.V., and Srivastra, A.K. Effect of *Centella asiatica* on pentylenetetrazole-induced kindling, cognition and oxidative stress in rats. Pharmacology, Biochemistry and Behavior 74 (2003): 579-585.

(31) Kumar, M.V. and Gupta, Y. Effect of Centella asiatica on cognition and oxidative stress in an intracerebroventricular streptozotocin model of alzheimer's disease in rats. Clinical and Experimental Pharmacology and Physiology 30 (2003): 336-342.

(32) Steenkamp, V. and Gouws, M.C. Cytotoxicity of six South African medicinal plant extracts used in the treatment of cancer. South African Journal of Botany 72 (2006): 630-633.

(33) Hussin, M., et al. Protective effect of *Centella asiatica* extract and powder on oxidative stress in rats. Food Chemistry 100 (2007): 535-541.

(34) Ghanapragasam, A., Ebenezar, K.K., Sathish, V., Govindaraju, P., and Devaki, T. Protective effect of *Centella asiatica* on antioxidant tissue defense system against adriamycin induced cardiomyopathy in rats. Life Science 76 (2004): 585-597.

(35) Hamid, A.A., Shah, Z.M., Muse, R., and Mohamed, S. Characterisation of antioxidative activities of various extracts of *Centella asiatica* (L) Urban. Food Chemistry 77 (2002): 465-469.

(36) Huda-Faujan, N., Noriham, A., Norrakiah, A.S., and Babji, A.S. Antioxidative activities of water extracts of some Malaysian herbs. Food Journal 14(1) (2007): 61-68.

(37) Jayashree, G., Muraleedhara, G.K., Sudarslal, S., and Jacob, V.B. Anti-oxidant activity of *Centella asiatica* on lymphoma-bearing mice. Fitoterapia 2003 (2003): 431-434.

(38) Zainol, M.K., Abd-Hamid, A., Yusof, S., and Muse, R. Antioxidative activity and phenolic compounds of leaf, root and petiole of four accessions of *Centella asiatica* (L.) Urban. Food Chemistry 81 (2003): 575-581.

(39) Inamdar, P.K., Yeole, R.D., Ghogare, A.B., and Souza, N.J.d. Determination of biologically active constituents in *Centella asiatica*. Journal of Chromatography A 742 (1996): 127-130.

(40) Shukla, A., et al. In vitro and in vivo wound healing activity of asiaticoside isolated from *Centella asiatica*. Journal of Ethnopharmacology 65 (1999): 1-11.

(41) Shukla, A., Rasik, A.M., and Dhawan, B.N. Asiaticoside-induced elevation of antioxidant levels in healing wounds. Phytotherapy Research 13(1) (1999): 50-4.

(42) Wijeweera, P., Arnason, J.T., Koszycki, D., and Merali, Z. Evaluation of anxiolytic properties of Gotukola- (*Centella asiatica*) extracts and asiaticoside in rat behavioral models. Phytomedicine 13 (2006): 668-676.

(43) Voet, D., Voet, J.G., and Pratt, C.W., Fundamental of Biochemistry. 2 ed., Asia: John Wiley & Sons. Inc, 2006.

(44) Valko, M., Rhodes, C.J., Moncol, J., Izakovic, M., and Mazur, M. Free radicals, metals and antioxidants in oxidative stress-induced cancer. Chemico-Biological interactions 160 (2006): 1-40.

(45) Valko, M., et al. Free radicals and antioxidants in normal physiological functions and human disease. The International Journal of Biochemistry & Cell Biology 39 (2007): 44-84.

(46) Batandier, C., Fontaine, E., Keriel, C., and Leverve, X.M. Determination of mitochondrial reactive oxygen species: methodological aspects. Journal of Cellular and Molecular Medicine 6(2) (2002): 175-187.

(47) Brookes, P.S. Mitochondrial H^+ leak and ROS generation: An odd couple. Free Radical Biology and Medicine 38 (2005): 12-23.

(48) Cadenas, E. Mitochondrial free radical production and cell signaling. Molecular Aspects of Medicine 25 (2004): 17-26.

(49) Muller, F.L., Liu, Y., and Rommen, H.V. Complex III releases superoxide to both sides of the inner mitochondrial membrane. Journal of Biological Chemistry 279(47) (2004): 49064-49073.

(50) Marnett, L.J. Lipid peroxidation - DNA damage by malonaldehyde. Mutation Research 424 (1999): 83-95.
(51) Poli, G. and Schaur, R.J. 4-Hydroxynonenal in the pathomechanisms of oxidative stress. IUBMB Life 50(4-5) (2000): 315-21.
(52) Stadtman, E.R. Role of oxidant species in aging. Current Medicinal Chemistry 11 (2004): 1105-1112.
(53) Gardner, H.W. and Hamberg, M. Oxygenation of (3Z)-nonenal to (2E)-4-hydroxy-2-nonenal in the broad bean (Vicia faba L.). Journal of Biological Chemistry 268(10) (1993): 6971-7.
(54) Gardner, H.W. and Grove, M.J. Soybean lipoxygenase-1 oxidizes 3Z-nonenal. A route to 4s-hydroperoxy-2e-nonenal and related products. Plant Physiology 116(4) (1998): 1359-66.
(55) Schneider, C., Tallman, K.A., Porter, N.A., and Brash, A.R. Two distinct pathways of formation of 4-hydroxynonenal. Mechanisms of nonenzymatic transformation of the 9- and 13-hydroperoxides of linoleic acid to 4-hydroxyalkenals. Journal of Biological Chemistry 276(24) (2001): 20831-8.
(56) Kinter, M. and Robert, R.J. Glutathione consumption and glutathione peroxidase inactivation in fibroblast cell lines by 4-hydroxy-2-nonenal. Free Radical Biology and Medicine 21(4) (1996): 457-462.
(57) Vieira, O., et al. Oxidized LDLs alter the activity of ubiquinatin-proteasome pathway: potential role in oxidized LDL-induced apoptosis. FASEB Journal 14 (2000): 532-542.
(58) Malecki, A., Garrido, R., Mattson, M.P., Hennig, B., and Toborek, M. 4-Hydroxynonenal induces oxidative stress and death of cultured spinal cord neurons. Journal of neurochemistry 74 (2000): 2278-2287.
(59) Elmore, S. Apoptosis: A Review of Programmed Cell Death. Tocicologic Pathology 35(4) (2007): 495-516.
(60) Kalinich, J.F., Ramakrishnan, R., McClain, D.E., and Ramakrishnan, N. 4-Hydroxynonenal, an end-product of lipid peroxidation, induces apoptosis in human leukemic T- and B-cell lines. Free Radical Research 33(4) (2000): 349-58.
(61) Jian, X., Ji-lin Zhou, Ning-fu Wang, and Xu, H.-y. Effects of 4-hydroxy-2-nonenal on cultured human aortic endothelial cells and myocardial cell. Engineer in Medicine and Biology 27th Annual Conference, Shanghai, China, 2005.
(62) Kutuk, O., Poli, G., and Basaga, H. Resveratrol protects against 4-hydroxynonenal-induced apoptosis by blocking JNK and c-JUN/AP-1 signaling. Toxicological Sciences 90(1) (2006): 120-132.
(63) Soh, Y., et al. Selective activation of the c-Jun N-terminal protein kinase pathway during 4-hydroxynonenal-induced apoptosis of PC12 cells. Molecular Pharmacology 58 (2000): 535-541.
(64) Liu, W., et al. 4-hydroxynonenal induces a cellular redox status-related activation of the caspase cascade for apoptotic cell death. Journal of Cell Science 113 (Pt 4) (2000): 635-41.
(65) Ji, C., Amarnath, V., Pietenpol, J.A., and Marnett, L.J. 4-hydroxynonenal induces apoptosis via caspase-3 activation and cytochrome c release. Chemical Research in Toxicology 14(8) (2001): 1090-6.

(66) Arakawa, M., et al. N-acetylcysteine selectively protects cerebellar granule cells from 4-hydroxynonenal-induced cell death. Neuroscience Research 55(3) (2006): 255-263.

(67) Whiteside, G., Cougnon, N., Hunt, S.P., and Munglani, R. An improved method for detection of apoptosis in tissue sections and cell culture, using the TUNEL technique combined with Hoechst stain. Brain Research Protocols 2(2) (1998): 160-164.

(68) Vitale, M., Zamai, L., Mazzotti, G., Cataldi, A., and Falcieri, E. Differential kinetics of propidium iodide uptake in apoptotic and necrotic thymocytes. Histochemistry and Cell Biology 100(3) (1993): 223-229.

(69) Zhang, Y., et al. The origin of reactive oxygen species in adrenocorticotropic hormone-induced hypertension in the rat. American Journal of Hypertension 17(5, Supplement 1) (2004): S75-S75.

(70) Nishikawa, T., et al. Impact of mitochondrial ROS production on diabetic vascular complications. Diabetes Research and Clinical Practice 77(3, Supplement 1) (2007): S41-S45.

(71) Schaefer, C.A., et al. Statins inhibit hypoxia-induced endothelial proliferation by preventing calcium-induced ROS formation. Atherosclerosis 185(2) (2006): 290-296.

(72) Kibel, A., Belovari, T., and Drenjancevic-Peric, I. The role of transferrin in atherosclerosis. Medical Hypotheses 70(4) (2008): 793-797.

(73) Miike, T., et al. Effects of an anti-oxidative ACAT inhibitor on apoptosis/necrosis and cholesterol accumulation under oxidative stress in THP-1 cell-derived foam cells. Life Sciences 82(1-2) (2008): 79-84.

(74) Chowdhry, M.F., Vohra, H.A., and Galiøanes, M. Diabetes increases apoptosis and necrosis in both ischemic and nonischemic human myocardium: Role of caspases and poly-adenosine diphosphate-ribose polymerase. The Journal of Thoracic and Cardiovascular Surgery 134(1) (2007): 124-131.e3.

(75) Abdelwahid, E. and Smith, G. Apoptosis in chronic heart failure. International Journal of Cardiology 114(3) (2007): 375-375.

(76) Degenhardt, K., et al. Autophagy promotes tumor cell survival and restricts necrosis, inflammation, and tumorigenesis. Cancer Cell 10(1) (2006): 51-64.

(77) Denecker, G., Vercammen, D., Declercq, W., and Vandenabeele, P. Apoptotic and necrotic cell death induced by death domain receptors. Cellular and Molecular Life Sciences (CMLS) 58(3) (2001): 356-370.

(78) Reid, S., Cross, R., and Charles Snow, E. Combined Hoechst 33342 and merocyanine 540 staining to examine murine B cell cycle stage, viability and apoptosis. Journal of Immunological Methods 192(1-2) (1996): 43-54.

(79) Maher, S. and McClean, S. Melittin exhibits necrotic cytotoxicity in gastrointestinal cells which is attenuated by cholesterol. Biochemical Pharmacology 75(5) (2008): 1104-1114.

APPENDICES

APPENDIX A
PREPARATION OF REAGENTS

4-HNE stock solution

To prepare a stock solution 10 mM, 31.24 µl of 4-HNE (32.0102 mM) was diluted with 68.76 µl of DMSO (used within 3 months).

Asiaticoside stock solution

To prepare a stock solution 12.5 mM, asiaticoside powder 6 mg was solubilized well in PBS 500 ml.

MTT solution

To prepare MTT solution at concentration 48.27 mM, MTT powder 3 mg was solubilized well in DMSO 150 µl.

Hoechst 33342 stock solution

To prepare a stock solution 5 mM, Hoechst 33342 powder 3.08 mg was solubilized well in PBS 1 ml.

PI stock solution

To prepare a stock solution 5 mM, PI powder 3.34 mg was solubilized well in PBS 1 ml.

$DCFH_2$-DA stock solution

To prepare a stock solution 5 mM, $DCFH_2$-DA powder 2.43 mg was solubilized well in DMSO 1 ml.

APPENDIX B
POSTER PRESENTATION

This research work was presented as a poster presentation, entitled PROTECTIVE EFFECTS OF ASIATICOSIDE AGAINST 4-HYDROXYNONENAL INDUCED ECV-304 CELL DAMAGE, at 4th BUU Grad. Research Conference, Burapha University, Chonburi, on March 13th, 2009. The poster numbers of participants was P-063.

Protective effects of asiaticoside against 4-hydroxynonenal induced ECV-304 cell damage.

Visarut Buranasudja[1], Pithi Chanvorachote[1], Rupporn Kittiwatchara[1], Vimolmas Lipipun[2]
[1]Department of Pharmacology and Physiology, [2]Department of Biochemistry and Microbiology,
Faculty of Pharmaceutical Sciences, Chulalongkorn University, Bangkok, Thailand.

INTRODUCTION

4-HNE, the most abundant aldehyde product of lipid peroxidation, was shown to exert several effects on pathological processes including, artherosclerosis and vasculitis. Its effects were shown to be associated with an ability to induce intracellular reactive oxygen species (ROS) generation (Uchida, 2003).

Asiaticoside, a major active compound found in *Centella asiatica* (L.) urban (Umbelliferae), has been shown to enhance antioxidant levels (Shukla, et. al., 1999). However, effects and mechanisms regarding asiaticoside in protection 4-HNE-induced endothelial cells death are still unknown.

In the present study, we elucidate the effects of 4-HNE and its underlying mechanisms in endothelial cell ECV-304. Additionally, we studied the protective effect of asiaticoside against 4-HNE toxicity in these cells.

MATERIALS & METHODS

Cell Culture and reagents

Human umbilical vein endothelial (ECV-304) cells were obtained from the American Type Culture Collection (Rockville, MD). Cells were cultured in DMEM medium, containing 5% fetal bovine serum, 2 mmol/L L-glutamine, and 100 units/ml penicillin/streptomycin in a 5% CO_2 environment at 37 °C.

Cytotoxicity assay

Cytotoxicity was determined by MTT colorimetric assay. Cells in 96-well plates were treated with substances for 24 hour and then incubated with 500 µg/mL of MTT for 4 hour at 37 °C. The intensity of the MTT product was measured at 550 nm using a microplate reader.

ROS Detection

Intracellular ROS generation was determined by flow cytometric analysis using the ROS-specific $DCFH_2$-DA. Briefly, cells were loaded with the probe (10 µM) for 30 min at 37 °C prior to treatment with substances for 1 hour. Fluorescence intensity was analyzed by flow cytometry using a 488-nm excitation beam and a 538-nm band-pass filter with CellQuest software.

RESULTS & DISCUSSION

1. 4-HNE induces cell death in endothelial ECV- 304 cells and its pro-oxidant effect.

To investigate the role of 4-HNE, endothelial cells were treated with various concentrations of 4-HNE (0-40 µM) and cell viability was determined after 24 hour by MTT assay. 4-HNE treatment caused dose-dependent decrease in cell survival as compared to untreated control (Figure 1). We also investigated whether 4-HNE had an ability to up-regulate ROS in these cells. The treatment of 4-HNE increased intracellular ROS level as shown in Figure 2.

2. Antioxidants inhibit 4-HNE induced toxicity in ECV-304 cells.

To provide supporting evidence for the involvement of ROS in the 4-HNE cytotoxicity, we treated endothelial cells with the toxic concentration of 4-HNE in the presence or absence of antioxidants and analyzed for cell survival by MTT assay. 4-HNE (20 µM) significantly decreased cell viability as compared to untreated control. Addition of antioxidant, NAC or GSH, strongly inhibited 4-HNE induced cytotoxicity, suggesting the involvement of ROS on this process (Figure 3).

3. Asiaticoside protects against 4-HNE induced ECV-304 cell death.

ECV-304 were co-treated with various concentrations of asiaticoside (0-200 µM) and toxic concentration of 4-HNE (20 µM). The asiaticoside significantly attenuated cytotoxic effect caused by 4-HNE (Figure 4). These data indicated that asiaticoside has a promising vascular protective effect which may be developed to be used in the vascular disease therapy.

Figure 1.

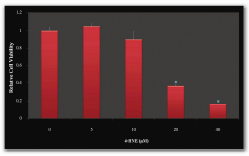

Figure 2.

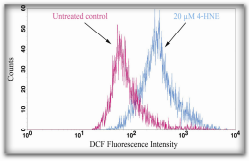

Figure 3.

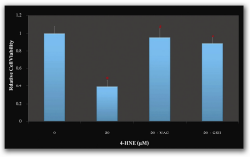

Figure 4.

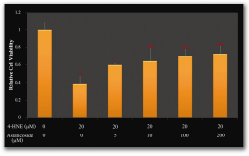

References

1. Shukla, A., Rasik, A. M., Dhawan, B.N.(1999). Asiaticoside-induced elevation of antioxidant levels in healing wounds. *Phyto Res, 13*(1), 50-54.

2.Uchida, K. (2003) 4-Hydroxy-2-nonenal: a product and mediator of oxidative stress. *Prog Lipid Res, 42*(4), 318-343.

Acknowledgements

The authors are grateful to **Dr. Surachai Unchen** (Faculty of Pharmacology and Physiology, Faculty of Pharmaceutical Sciences, Chulalongkorn University).

This research was supported by the Graduate Thesis Grant, Chulalongkorn University.

ฝ่ายบัณฑิตศึกษา มหาวิทยาลัยบูรพา

มอบเกียรติบัตรนี้แด่

คุณวิศรุต บูรณสัจจะ

ในโอกาสที่ได้นำเสนอผลงานวิจัย (แบบโปสเตอร์)

ในงาน

การนำเสนอผลงานวิจัยระดับบัณฑิตศึกษา ครั้งที่ 4

ณ มหาวิทยาลัยบูรพา, บางแสน จังหวัดชลบุรี

13 มีนาคม 2552

รองศาสตราจารย์ ดร.ประทุม ม่วงมี

รองอธิการบดีฝ่ายบัณฑิตศึกษา

มหาวิทยาลัยบูรพา

Vita

Mr. Visarut Buranasudja was born on May 12, 1984 in Bangkok. He received his B.Sc. in Pharmacy (1^{st} class honor) from the Faculty of Pharmaceutical Sciences, Chulalongkorn University in 2006. Currently, he works as an instructor of Department of Pharmacology and Physiology, Faculty of Pharmaceutical Sciences, Chulalongkorn University.